

Article

Very-low-protein diets lead to reduced food intake and weight loss, linked to inhibition of hypothalamic mTOR signaling, in mice

Yingga Wu,^{1,2,3} Baoguo Li,^{1,2} Li Li,^{1,2} Sharon E. Mitchell,³ Cara L. Green,³ Giuseppe D'Agostino,³ Guanlin Wang,^{1,2,3} Lu Wang,^{1,2,3} Min Li,^{1,2,3} Jianbo Li,⁴ Chaoqun Niu,¹ Zengguang Jin,⁴ Anyongqi Wang,^{1,2} Yu Zheng,^{1,2} Alex Douglas,³ and John R. Speakman^{1,3,5,6,7,*}

¹State Key Laboratory of Molecular Developmental Biology, Institute of Genetics and Developmental Biology, Chinese Academy of Sciences, Beijing 100101, PRC

²University of Chinese Academy of Sciences, Shijingshan District, Beijing 100049, PRC

³Institute of Biological and Environmental Sciences, University of Aberdeen, Aberdeen AB24 2TZ, Scotland, UK

⁴University of Dali, Dali, Yunnan 671000, PRC

⁵Center for Energy Metabolism and Reproduction, Shenzhen Institutes of Advanced Technology, Chinese Academy of Sciences, Shenzhen, PRC

⁶CAS Center of Excellence in Animal Evolution and Genetics, Kunming, PRC

⁷Lead contact

*Correspondence: j.speakman@abdn.ac.uk

<https://doi.org/10.1016/j.cmet.2021.01.017>

SUMMARY

The protein leverage hypothesis predicts that low dietary protein should increase energy intake and cause adiposity. We designed 10 diets varying from 1% to 20% protein combined with either 60% or 20% fat. Contrasting the expectation, very low protein did not cause increased food intake. Although these mice had activated hunger signaling, they ate less food, resulting in decreased body weight and improved glucose tolerance but not increased frailty, even under 60% fat. Moreover, they did not show hyperphagia when returned to a 20% protein diet, which could be mimicked by treatment with rapamycin. Intracerebroventricular injection of AAV-S6K1 significantly blunted the decrease in both food intake and body weight in mice fed 1% protein, an effect not observed with inhibition of eIF2a, TRPML1, and Fgf21 signaling. Hence, the 1% protein diet induced decreased food intake and body weight via a mechanism partially dependent on hypothalamic mTOR signaling.

INTRODUCTION

There is continuing debate about how food macronutrient composition relates to body weight control. Many previous studies emphasized fat and carbohydrates (Schutz, 1995), but recently, a role for protein was emphasized in the protein leverage hypothesis (Simpson and Raubenheimer, 2012). This idea suggests animals ingest food primarily to meet a protein target, and hence predicts overconsumption of energy, positive energy balance, and obesity as dietary protein levels decline. In mice, we found no significant correlation between energy intake or body composition when dietary protein content varied between 5% and 30% (Hu et al., 2018). This contrasts with other studies that suggested dietary protein content drives intake and adiposity (Keller, 2011; Huang et al., 2013; Solon-Biet et al., 2014). However, this may be more a difference of degree than a fundamentally different outcome. Since there was a small increase in food intake in mice eating the lowest protein levels in our previous study (Hu et al., 2018), it is possible we did not extend the protein content low enough to reveal the full impacts of protein on intake and adiposity.

Dietary protein comprises both essential and non-essential amino acids. Among the essential amino acids, leucine, isoleucine, and valine are called branched-chain amino acids (BCAA). Deprivation of leucine in mice caused decreased adiposity by stimulation of lipolysis in white adipose tissue (WAT) and upregulation of UCP-1 in brown adipose tissue (Cheng et al., 2010). Restriction of methionine caused several behavioral, physiological, and biochemical responses that improved metabolic health and increased longevity in rodents (Orgeron et al., 2014; Yang et al., 2019). Decreased consumption of BCAA was indicated to have a positive effect on metabolic health primarily by improving glucose tolerance (Fontana et al., 2016). These effects of low dietary levels of essential amino acids, however, contrast with the predicted effects from the protein leverage hypothesis, since at low amino acid levels adiposity was decreased. This may be because only individual amino acids were restricted rather than total protein levels.

Energy intake is mainly regulated by neuropeptides and signaling molecules in the hypothalamus. Four important "canonical" neuropeptides are neuropeptide Y (*Npy*), agouti-related peptide (*AgRP*), pro-opiomelanocortin (*Pomc*), and cocaine and



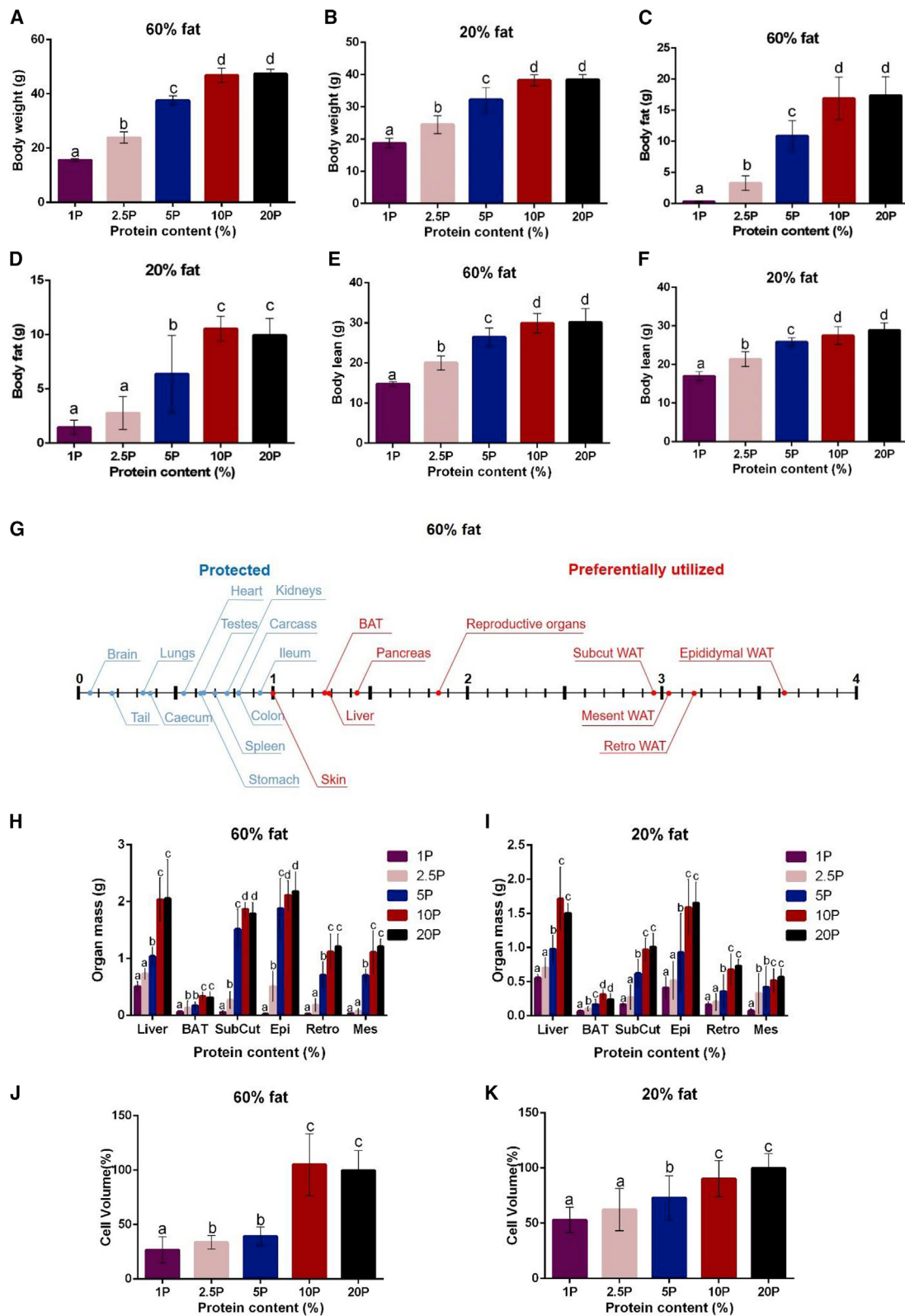


Figure 1. Body composition and cell size changes of mice treated with variable protein content and fixed 60% and 20% fat diets, respectively
(A and B) Average body weight of the last 10 days of measurement ($n = 13-16$).
(C-F) (C and D) Average fat weight and (E and F) average lean weight during last week of measurement ($n = 13-16$).

amphetamine-regulated transcript (*Cart*). Increased expression of *Npy* and *AgRP* stimulate food intake, whereas upregulation of *Pomc* and *Cart* cause reduced food intake (Ahima and Antwi, 2008; Schwartz et al., 2000; Wilding, 2002). Leptin and insulin interact with these neuropeptides. The mammalian target of rapamycin (mTOR) is also important in the process of food-intake regulation by the hypothalamus (Cota et al., 2006; Varela et al., 2012). Usually, mTOR expression is increased under energy surplus. Intracerebroventricular (ICV) leptin injection induces mTOR activation, leading to food-intake reduction and weight loss (Cota et al., 2006); mTOR also responds to amino acids (Beugnet et al., 2003; Carroll et al., 2016; Jewell et al., 2015; Wang et al., 2015). In a recent study, S6K1 in the hypothalamus was shown to regulate energy expenditure in mice fed a diet deprived of essential amino acids (Xia et al., 2012).

In this study, we designed diets with protein contents varying from 1% to 20% combined with either 60% or 20% fat. We characterized the responses to these diets in C57BL/6N male mice. Mice were introduced to the diets at 16 weeks of age, approximately equivalent to early human adulthood (Somerville et al., 2004), thereby avoiding impacts on developmental processes. We explored the mechanisms by which low protein exerts its effects on energy balance and body composition, fatty acid and amino acid metabolism, leptin sensitivity, and, especially, hypothalamic gene expression.

RESULTS

Unless otherwise stated, when we refer to “low-protein” groups this refers to mice fed 1%, 2.5%, or 5% protein.

Low protein caused decreased body weight even with 60% fat

There was no significant difference in body weight among all groups before exposure to the variable protein diets ($p = 0.619$ for the 60% fat group and $p = 0.412$ for the 20% fat group). After 12 weeks dietary treatment, body weight, fat weight, and lean weight were all significantly positively correlated with dietary protein content ($p < 0.001$ for both 60% and 20% dietary fat groups) (Figures 1A–1F). Body weight over the final 10 days of measurement in the low-protein groups was significantly lower than the 10% and 20% protein groups (ANOVA with post hoc Tukey’s test: $p < 0.001$ for 60% and 20% dietary fat groups for all comparisons) (Figures 1A and 1B). The fat and lean weight changes were almost identical to the body weight changes (Figures 1C–1F). The low-protein groups had significantly reduced fat and lean weight compared with the 20% protein group irrespective of the fat content of the diet (ANOVA with post hoc Tukey’s test: $p < 0.001$), and average body weight over the entire 12 weeks showed the same pattern (Figures S1A–S1D). Of

note, mice fed the 1% protein and 60% fat diet had very low fat weight (0.32 ± 0.096 g) after 12 weeks treatment.

The detailed organ level analysis showed that the liver, pancreas, all the white adipose tissue depots, brown adipose tissue, and the reproductive organs preferentially contributed to the weight loss ($\beta > 1$). In contrast, the vital organs, including the brain, heart, kidneys, lungs, and alimentary tract, were protected ($0 < \beta < 1$) (Figure 1G; Table S1). This effect was similar for the 60% fat and 20% fat groups (Table S1; Figure S1E). If the absolute weight of livers and adipose tissues are considered, the low-protein groups had significantly lower liver, subcutaneous, epididymal, retroperitoneal and mesenteric WAT, and brown adipose tissue weights (p values in Table S6) (Figures 1H and 1I). Hence, the mice mainly utilized fat tissues and their livers during weight loss and protected other lean tissues. Hematoxylin-eosin (HE) staining of white adipocytes indicated that cell volume in the low-protein groups was significantly reduced ($p < 0.001$ for all comparisons compared with the 20% protein group). For example, the 1% protein 60% fat group had a 40% reduction in cell volume compared with the 20% protein 60% fat group (Figures 1J, 1K, and S1F). Oil red staining indicated that low-protein groups had reduced lipid droplets in hepatocytes (Figure S1G). These patterns were the same in both the 60% and 20% fat groups (Figures S1F and S1G).

Fatty acid metabolism and amino acid metabolic pathways were changed in the liver and fat tissues during protein restriction

To investigate whether the reduced adipocyte cell volume and liver lipid droplets in the low-protein groups were the result of reduced lipogenesis and the increased fatty acid β -oxidation, we examined the expression levels of mRNAs related to these processes in each tissue. Fatty acid synthesis genes, fatty acid synthase (*Fas*), acetyl CoA carboxylase 1 (*Acc1*), and stearoyl CoA desaturase (*Scd1*) were significantly downregulated (Figure 2A), and in contrast, fatty acid β -oxidation genes fatty acyl-CoA oxidase (*Acox1*) and carnitine palmitoyltransferase 1 (*Cpt1*) were significantly upregulated (Figure 2B) in the livers of the low-protein groups irrespective of the dietary fat content (Figures S2A and S2B) (p values in Table S7) when compared with the 20% protein groups. However, in the white adipose tissue, there were no significant differences in gene expression of the fatty acid synthesis genes *Fas*, *Acc1*, and *Scd1* between the low-protein groups and 20% protein group ($p > 0.05$) (Figures 2C and S2C). Fatty acid oxidation genes *Acox1* and *Cpt1* were significantly elevated in white adipose tissues of the low-protein groups compared with the 20% protein group, except there was no significant difference in *Acox1* and *Cpt1* expression between the 5% and 20% protein groups under 60% fat (Figures 2D and S2D) (p values in Table S7). Fibroblast growth factor 21 (*Fgf21*)

(G) The gradient of linear least-squares regression equation between logged final body weight and the final organ weight to express the relative utilization of each tissue in the 60% fat group. Values less than 1 reflect the protection of the tissue and values greater than 1 indicate disproportional utilization during weight loss ($n = 11\text{--}13$).

(H and I) Organ sizes of the liver, BAT, brown adipose tissue; SubCut, subcutaneous; Epi, epididymal; Retro, retroperitoneal; and Mes, mesenteric white adipose tissue ($n = 11\text{--}13$).

(J and K) Calculation of white adipose cell size by ImageJ to express the relative cell-size decrease. We defined the cell size of 20% protein group as 100% reference ($n = 5$). One-way ANOVA was performed for statistical analysis for (A–F) and (H–K). Differences with $p < 0.05$ were considered significant, groups with the same letter were not significantly different ($p > 0.05$). Values are represented as mean \pm SD. See also Figure S1; Table S1.

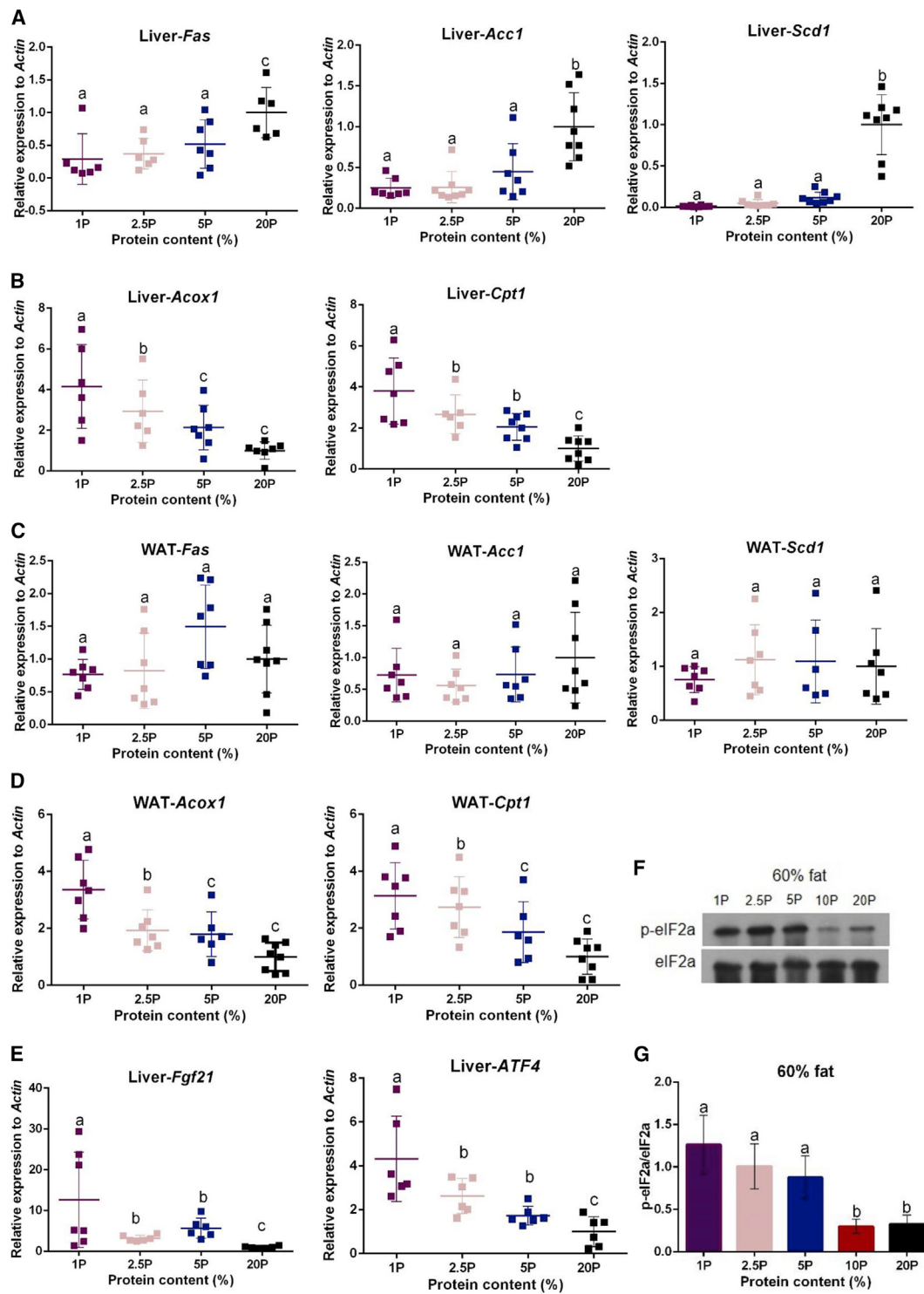


Figure 2. The changes of gene expression in fatty acid and amino acid metabolism pathways in the liver and white adipose tissues after 12 weeks treatment of variable protein content and fixed 60% fat diets

(A–D) Relative mRNA expressions of fatty acid synthesis genes (*Fas*, *Acc1*, and *Scd1*) and fatty acid oxidation genes (*Acox1* and *Cpt1*) to β -actin (A and B) in liver tissues and (C and D) in white adipose tissue ($n = 6$ –8).

(E) Relative mRNA expressions of *ATF4* and *Fgf21* to β -actin in the liver ($n = 6$ –7).

(F and G) Western blotting result and quantification of p-eIF2 α protein expression in liver ($n = 3$). One-way ANOVA was performed for statistical analysis. Differences with $p < 0.05$ were considered to be significant, and groups with the same letter were not significantly different ($p > 0.05$). Values are represented as mean \pm SD. See also Figure S2.

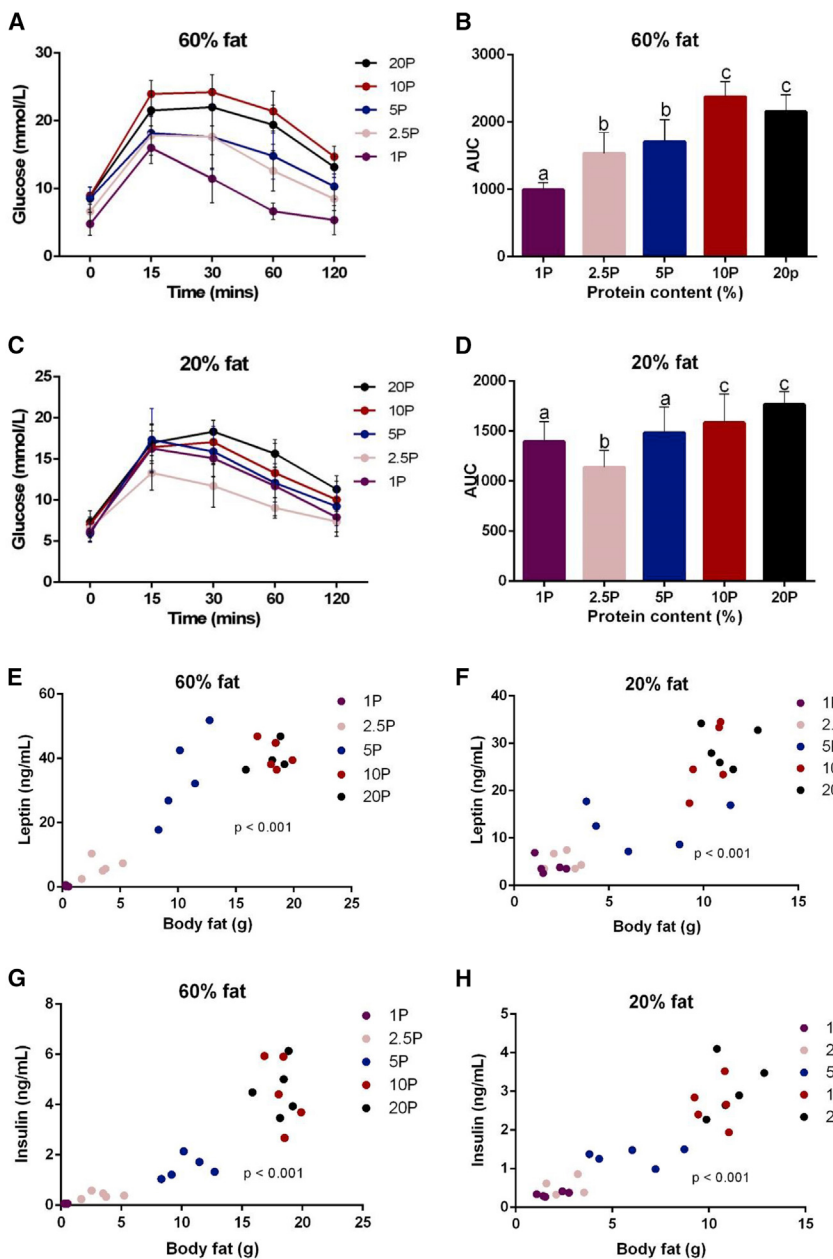


Figure 3. Glucose tolerance test of mice after 8 weeks, and serum leptin and insulin concentrations of mice after 12 weeks, on the diets with variable protein content and fixed 60% fat and 20% fat, respectively

(A and B) Blood glucose levels after 0, 15, 30, 60, and 120 min of glucose injection in each group ($n = 7-9$).

(C and D) AUC in (A and B) ($n = 7-9$).

(E-H) Regression between body fat and serum leptin concentration (E and F) and serum insulin concentration (G and H) ($n = 5$ mice per group). For (B and D), one-way ANOVA was performed for statistical analysis. Differences with $p < 0.05$ were considered to be significant, groups with the same letter were not significantly different ($p > 0.05$). For (E-H), regression analysis was used, $p < 0.05$ was considered to be significant. Values are represented as mean \pm SD.

Analysis of covariance (ANCOVA) with fat weight as a covariate showed that the AUC was also significantly different among different protein content groups when corrected for fat weight effects. Serum leptin and insulin concentrations were significantly positively correlated with the body fat weight ($p < 0.001$) (Figures 3E–3H).

Low-protein diets did not increase frailty and improved memory performance

Grip strength and bone density were positively, and rotarod performance negatively, related to body weight ($p < 0.001$) (Figures S3A–S3C). Analysis of covariance (ANCOVA) with body weight as a covariate showed that there were no significant differences between different protein content groups for grip strength, rotarod performance, and bone density changes ($p > 0.05$). The 1% and 2.5% protein groups made

significantly fewer errors compared with the control group in the radial arm maze test (ANOVA with post hoc Tukey's test: $p = 0.023$ for 1% protein, and $p = 0.013$ for 2.5% protein) under a 20% low-fat condition. The 1% low protein 60% fat group were faster to complete the task compared with the control group (ANOVA with post hoc Tukey's test: $p = 0.014$) (Figures S3D–S3I). Overall lower dietary protein led to improved memory performance.

Different levels of low protein caused divergent effects on energy balance

There were significant differences between different protein content groups for gross energy intake under 60% or 20% fat (ANOVA: $p < 0.001$). Mice fed moderately low protein (5% protein group) ate slightly more food (gross energy intake)

was significantly increased in the liver in low-protein groups compared with the 20% protein group, independent of dietary fat content (Figures 2E and S2E) (p values in Table S7). Activating transcription factor 4 (ATF4) and downstream protein p-eIF2α were also significantly upregulated in the low-protein groups (Figures 2E–2G and S2E–S2G) (p values in Table S7).

Low dietary protein caused improved glucose tolerance

The low-protein groups had significantly decreased area under the curve (AUC) in the ipGTT (ANOVA with post hoc Tukey's test: $p = 0.015$ for 60% fat group and $p = 0.023$ for 20% fat group) compared with the 20% protein groups (Figures 3A–3D), whereas there was no significant difference in AUC between the 10% and 20% protein groups. Hence, low dietary protein improved glucose tolerance in mice even when fed 60% fat.

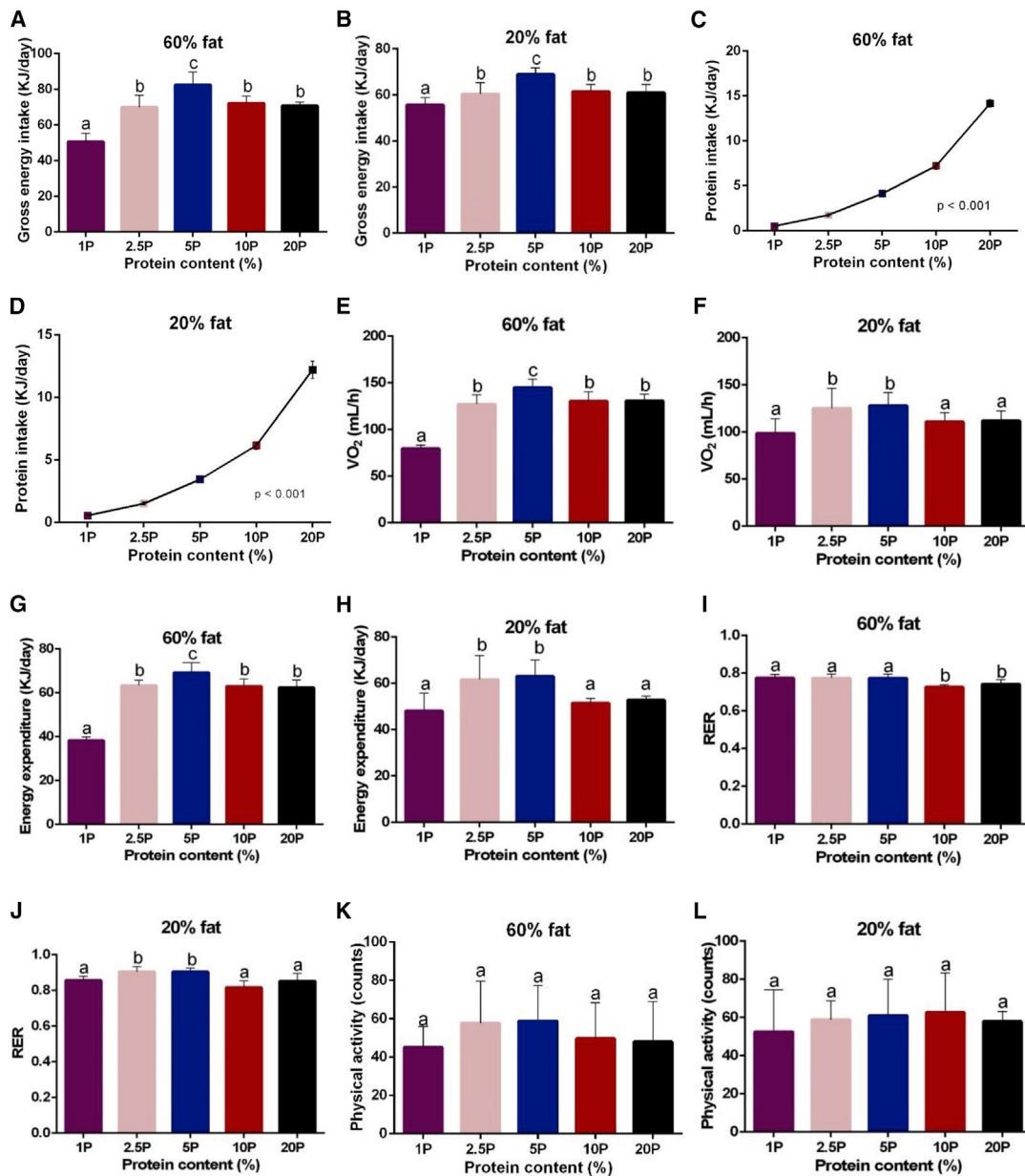


Figure 4. Changes of energy balance and metabolism of mice after a 12-week exposure to variable protein content and fixed 60% fat and 20% fat diets

(A and B) Average gross energy intake over the last 10 days of measurement ($n = 13\text{--}17$).

(C and D) Average protein intake over the last 10 days of measurement ($n = 13\text{--}17$).

(E and F) Average VO_2 (mL/h) consumption ($n = 5\text{--}8$).

(G and H) Average daily energy expenditure ($n = 5\text{--}8$).

(I and J) Average RER ($n = 5\text{--}8$).

(K and L) Average physical activity levels ($n = 5\text{--}8$). One-way ANOVA analysis was performed for statistical analysis, groups with the same letter were not significantly different and differences with $p < 0.05$ were considered to be significant. Values are represented as mean $\pm \text{SD}$. See also Figure S3.

compared with the 20% protein group (ANOVA with post hoc Tukey's test: $p < 0.001$ for 60% fat group). The gross energy intake of 2.5% protein group was not significantly different from the 20% protein group (ANOVA with post hoc Tukey's test: $p > 0.05$). The 1% protein group had significantly lower gross energy intake than the 20% protein group in both

60% and 20% fat groups (ANOVA with post hoc Tukey's test: $p < 0.001$) (Figures 4A and 4B). Gross daily energy intake was on average 28% lower in the 60% fat group and 10% lower in the 20% fat group, for mice fed 1% protein compared with 20% protein (Figures 4A and 4B). Patterns were the same for average gross energy intake over the entire 12 weeks

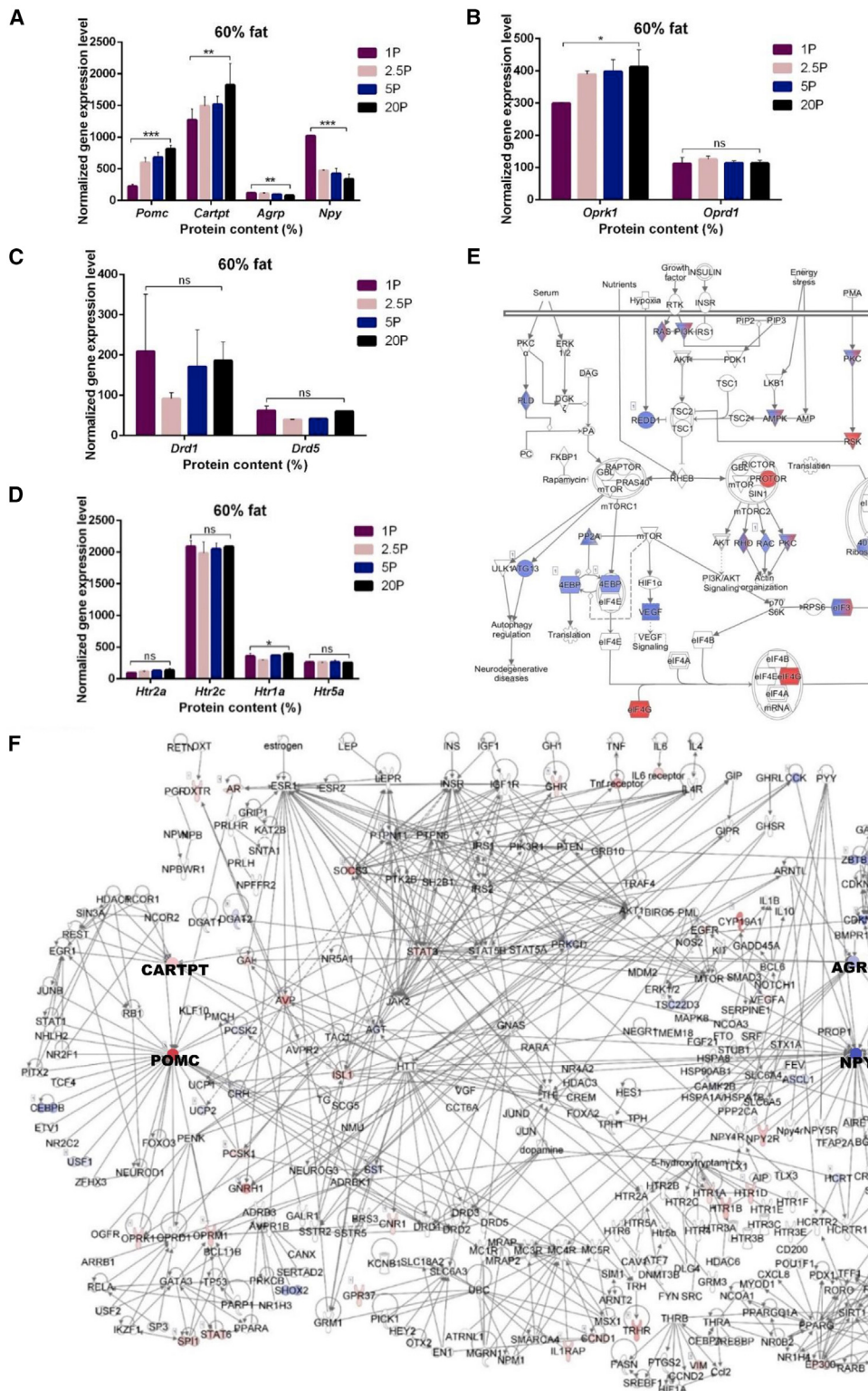


Figure 5. Pathway diagram showing GLM regression of gene expression against dietary protein contents and the expression levels of key hunger signaling and feeding-behavior-related genes in the hypothalamus of mice fed different protein content diets

(A–D) Gene-expression levels in (A) hunger signaling pathway, (B) dopamine signaling pathway, (C) opioid signaling pathway, and (D) serotonin receptor signaling pathway in different protein content and 60% fat diets fed mice.

(legend continued on next page)

(ANOVA: $p < 0.001$) (Figures S3J and S3K). Net energy intake also differed significantly between groups (ANOVA: $p < 0.01$). The pattern was similar to the gross energy intake changes (Figures S3L and S3M). Protein intake also differed between groups. Protein intake was significantly positively correlated with the protein content in the diet ($p < 0.001$ for all groups) (Figures 4C and 4D). Hence, the low-protein groups did not upregulate their total intake to sustain protein intake constant as expected for perfect leverage.

There were significant differences in both oxygen consumption and energy expenditure between mice fed different protein diets (ANOVA: $p < 0.001$, $p = 0.005$ for oxygen consumption and $p < 0.001$, $p = 0.001$ for energy expenditure changes in 60% fat and 20% fat group, respectively) (ANCOVA with body weight as covariate: $p < 0.001$, $p = 0.003$ for oxygen consumption and $p < 0.001$, $p < 0.001$ for energy expenditure under 60% fat and 20% fat conditions, respectively) (ANCOVA with fat free weight as covariate: $p < 0.001$, $p = 0.001$ for oxygen consumption and $p < 0.001$, $p < 0.001$ for energy expenditure changes for 60% fat and 20% fat respectively) (Figures 4E–4H). Under the 60% fat condition, only the 5% dietary protein group had significantly increased daily energy expenditure, compared with the 20% protein group (ANOVA with post hoc Tukey's test: $p = 0.012$), whereas under the 20% fat level, both 2.5% and 5% protein groups had significantly higher energy expenditure (ANOVA with post hoc Tukey's test: $p = 0.031$ and $p = 0.014$) relative to the 20% protein group (Figures 4G and 4H). In contrast, the 1% protein group at 60% fat had significantly decreased energy expenditure, due in part to their much lower body weight (ANOVA: $p < 0.01$) (Figure 4G). When we used body weight as a covariate in an ANCOVA analysis of daily energy expenditure (DEE), there were no significant differences between 5% protein and 20% protein under 60% fat condition and 2.5%, 5%, and 20% protein under 20% fat condition (ANCOVA: $p > 0.05$). The average oxygen consumption and the 24-h oxygen consumption changes mirrored the changes in energy expenditure (Figures 4E, 4F, S3N, and S3O). Respiratory exchange ratio (RER) in the 20% fat condition followed the pattern in oxygen consumption (ANOVA with post hoc Tukey's test: $p = 0.028$ and $p = 0.029$ for 2.5% and 5% protein groups compared with the 20% protein group), but for the 60% fat group, all the low-protein groups had significantly higher RER compared with the 20% protein group (ANOVA with post hoc Tukey's test: $p = 0.017$, 0.017, and 0.012 for 1%, 2.5%, and 5% groups, respectively) (Figures 4I and 4J). RER of high-fat groups averaged 0.76 ± 0.02 and was 0.87 ± 0.04 for the low-fat groups, consistent with fat being the predominant fuel source in the high-fat groups. There were no significant differences in physical activity between groups (ANOVA: $p > 0.05$) (Figures 4K and 4L). In summary, the 1% protein group had decreased fat and lean weight mostly because of decreased net energy intake compared with the 20% protein group. Energy expenditure declined in parallel with reduced body weight.

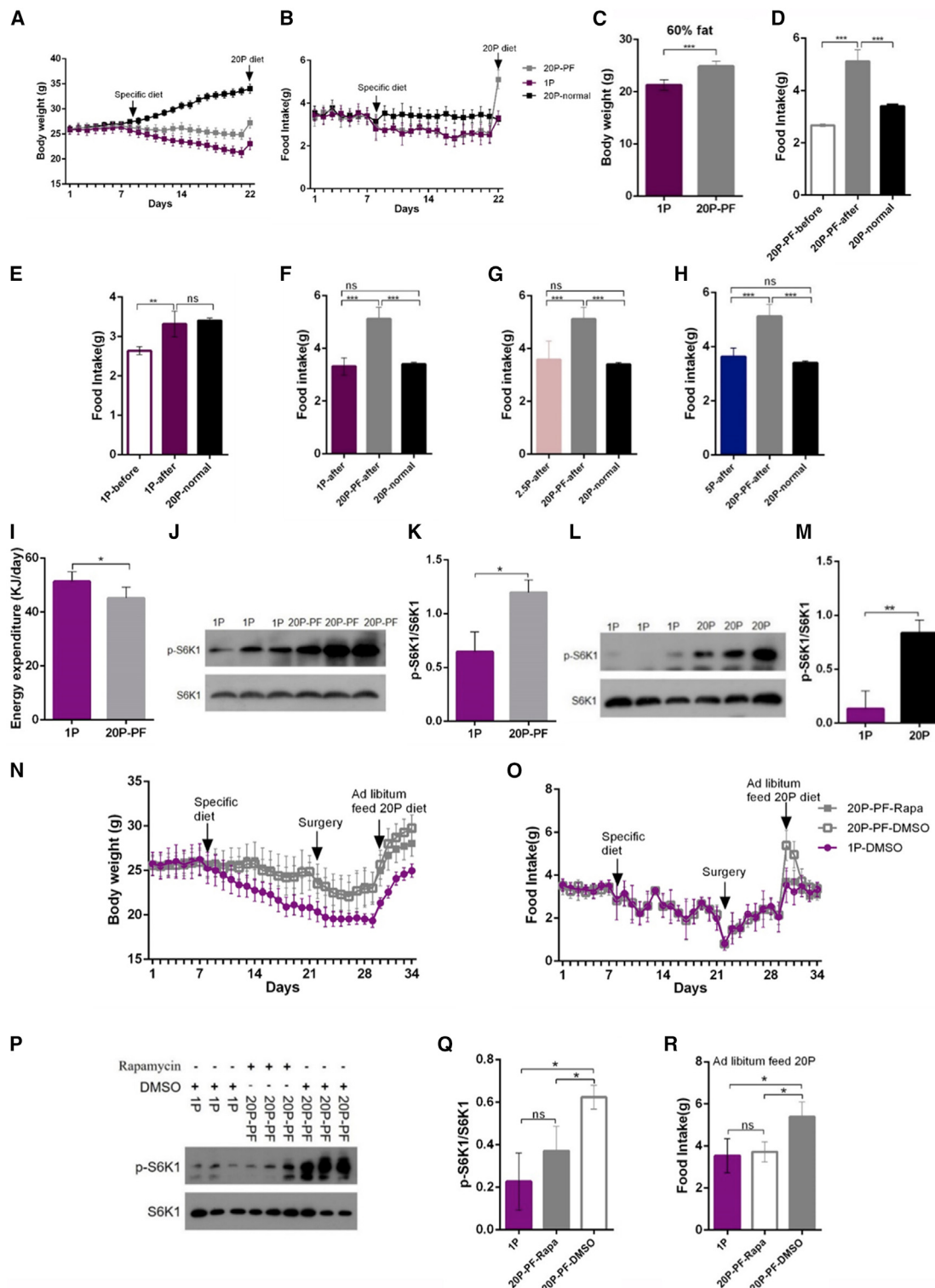
Hypothalamic hunger signaling was activated and mTOR signaling was inhibited by dietary low protein

To investigate if the lower food intake under lowered dietary protein contents was due to reduced signaling in the hunger-related pathways of the hypothalamus, and/or changes in other related pathways, we performed hypothalamic RNA sequencing (RNA-seq) analysis. The most affected pathways included the mTOR signaling pathway, the hunger signaling pathway, eIF2α signaling pathway, and regulation of eIF4 and p70S6K signaling pathways ($p = 5.26 \times 10^{-11}$, $p < 0.01$, $p = 5.51 \times 10^{-15}$, $p = 5.08 \times 10^{-10}$, respectively, for each pathway) (Figures 5E and 5F). There were 47 significant correlations with dietary protein content in hypothalamic gene expression in the mTOR signaling pathway, including 11 positive and 36 negatively correlated genes with dietary protein content (Figure 5E). In the hypothalamic hunger pathway, changes in 56 genes were significantly associated with dietary protein levels, most of which (36/56) had increased expression with increasing dietary protein (Figure 5F). In addition, expression of 56 genes in the eIF2α signaling pathway showed significant correlations to dietary protein changes, 42 of which were negatively and 14 positively correlated to dietary protein.

There were strong correlations for four key hunger signaling pathway genes *Pomc*, *Cart*, *Npy*, and *AgRP* with the protein content in the diet ($p = 2.2 \times 10^{-4}$ for *Pomc*, $p = 0.008$ for *Cart*, $p = 0.008$ for *AgRP* and $p = 8.77 \times 10^{-5}$ for *Npy*) with *Pomc* and *Cart* expression significantly reduced and *Npy* and *AgRP* expression increased as protein levels decreased (Figures 5A, S4A, S4E, and S4F). We found no significant effects of dietary protein on gene-expression levels of the hedonic signaling systems, including dopamine receptors (*Drd1*, *Drd5*) and opioid receptors (*Oprk1* and *Oprd1*) ($p > 0.05$), except *Oprk1* significantly increased with increasing dietary protein ($p = 0.039$) (Figures 5B, 5C, S4B, and S4C). The gene expressions of *Htr2a*, *Htr2c*, and *Htr5a* in the serotonin receptor signaling pathway were also not significantly affected by protein content in the diet ($p > 0.05$), whereas *Htr1a* was significantly positively related to dietary protein content ($p = 0.048$) (Figures 5D and S4D). Hence, the most significantly modulated pathways in the hypothalamus were the mTOR signaling pathway and the canonical hunger signaling pathway. Changes in the hunger signaling pathway indicated that mice under lower protein levels had stimulated rather than reduced hunger signaling, despite eating less food.

Mice under low-protein levels had low levels of serum leptin and stimulated hunger signaling pathways. To further explore the responses to exogenous leptin in mice fed different protein content diets, we injected phosphate buffer solution (PBS) or leptin to food-deprived mice in each group and observed the food intake changes 1, 3, and 4 h after PBS or leptin treatment. We found average 4-h food intakes were significantly decreased in 1% and 2.5% very-low-protein groups following leptin treatment compared with the PBS-treated mice ($p = 0.002$,

(E and F) Pathway diagrams for (E) mTOR signaling pathway and (F) hunger signaling pathway, red indicates positive and blue indicates the negative regression with the protein content in the diet, gray indicates no significance. Generalized linear modeling was performed to analyze the dietary protein effect on specific gene expression and pathway under 60% and 20% fat conditions. For (A–D), * $p < 0.05$, ** $p < 0.01$, *** $p < 0.001$, ns $p > 0.05$. Values are represented as mean \pm SD. Each group had 2 pooled samples from 6 individuals. See also Figure S4.

**Figure 6. Rapamycin blocked the hyperphagia effect of caloric restriction in mice**

(A and B) Body weight and food intake changes of 1% protein, 20% protein pair feeding, and 20% protein mice before and after *ad libitum* fed with 20% protein diet ($n = 8$), the mice were fed the baseline diet for 1 week and then treated, respectively, with 1% protein, 20% protein, and pair feeding 20% protein diet (special diet) for 2 weeks followed by treated with 20% protein diet.

(C) Average body weight changes of 1% protein and 20% protein pair feeding group in (A).

(legend continued on next page)

$p = 0.029$ for 60% fat and $p = 0.015$, $p = 0.005$ for 20% fat) (Figures S4G–S4J), but there were no significant differences between leptin and PBS for the average food intake changes over 4 h in the 5% and 20% protein groups ($p > 0.05$) (Figures S4G–S4J). The hypothalamic *Pomc* and *AgRP* gene-expression levels in these leptin-treated mice were consistent with the pattern of food-intake changes. That is, *Pomc* expressions were significantly upregulated ($p = 0.003$ and $p = 0.002$ for 1% and 2.5% protein groups respectively) and *AgRP* expressions were significantly downregulated ($p = 0.017$ and $p = 0.378$ for 1% and 2.5% protein group respectively) in leptin injected mice compared with the PBS injected mice, but no significant differences existed for these two gene-expression levels in 5% and 20% protein groups ($p > 0.05$) (Figures S4K–S4N). p-stat3 expressions were also significantly increased in 1% and 2.5% leptin-treated groups compared with the respective PBS-treated groups ($p = 0.031$ and $p = 0.048$ for 1% and 2.5% protein group) but not for the 5% and 20% protein groups (Figures S4O and S4P). Overall the very-low-protein groups with 1% and 2.5% dietary protein group had significantly increased leptin sensitivity.

Serum metabolome pathways related to weight loss were also activated by low dietary protein levels

Serum levels of aspartic acid and glycine were significantly negatively correlated with the dietary protein content ($p < 0.001$), whereas phenylalanine, tryptophan, leucine, isoleucine, and valine were all significantly positively correlated with dietary protein content ($p < 0.001$) (Figures S5B and S5C). General linear modeling across all metabolites and subsequent Ingenuity pathway analysis (IPA) results showed that the most affected pathways included tRNA charging, phenylalanine degradation, glutamate receptor signaling, glutamyl cycle, and citrulline-nitric oxide cycle ($p = 0.002$, $p = 0.008$, $p = 0.008$, $p = 0.03$, $p = 0.03$ respectively) (Table S2). There were 5/43 metabolites significantly changed in the tRNA charging pathway, including two metabolites that had negative and three metabolites with positive associations with dietary protein content (Figure S5D). Only 3/20 metabolites were significantly associated with protein levels in the phenylalanine degradation pathway: phenylalanine was positively correlated, whereas glutamine and glycine were negatively correlated, with dietary protein content (Figure S5A). Changes in the expression levels of 3/11 metabolites in the citrulline-nitric oxide cycle pathway were significantly correlated with dietary protein levels, 2 of which were negatively and 1 positively related to elevated dairy protein. Both in glutamate receptor signaling and glutamyl cycle signaling pathway, only 2 metabolites had significant correlations with dietary protein content (Figure S5E). We also performed Pearson correlations between all the metabolite expression levels and the dietary protein levels across the different protein groups and found that, apart from

these significantly changed pathways related to the dietary protein content in the generalized linear modeling (GLM) analysis, bupropion degradation and threonine synthesis pathways were also included in the significantly affected pathways (Table S2). In conclusion, several amino acids including BCAA, phenylalanine, tryptophan, aspartic acid, glycine, and metabolic pathways related to weight loss were significantly changed in the low-protein groups.

Protein-restricted mice did not show hyperphagia compared with pair-fed mice

Previous studies showed that if calorically restricted mice were given free access to food for 24 h, they showed hyperphagia. We fed a group of mice the 1% protein and 60% fat diet, and another group was pair-fed (by energy) to this group using the 20% protein and 60% fat diet for 2 weeks. Then all mice were given *ad libitum* access to the 20% protein 60% fat diet for 24 h and their food intakes were observed. After 2-weeks pair feeding treatment, the body weight of pair-fed group treated with 20% protein diet (20P-PF) was significantly higher than 1% protein group ($p = 4.05 \times 10^{-6}$) (Figures 6A–6C). Further, after *ad libitum* exposure to the 20% protein diet, the pair-fed group showed significant hyperphagia, compared with the intake of the control non-pair fed (normal 20% protein group) mice on the same diet (5.11 ± 0.44 g/day compared with 3.4 ± 0.07 g/day) ($p = 3.77 \times 10^{-6}$) (Figure 6D). In contrast, the 1% protein group increased their food intake compared with their 1% diet food intake (1% protein diet: 2.64 ± 0.11 g/day and 20% protein diet: 3.31 ± 0.33 g/day ($p < 0.001$), but they did not increase as much as the pair-fed mice did, and the 1% protein diet-fed mice did not eat more food after exposure to the 20% protein diet than the food intake of the normal 20% protein group (3.31 ± 0.33 g/day and 3.4 ± 0.07 g/day respectively) ($p > 0.05$) (Figure 6E). The food intake of 1% protein group was significantly lower than the 20% protein pair-fed group when we changed the diet to the *ad libitum* 20% protein diet (3.31 ± 0.33 g/day and 5.11 ± 0.44 g/day respectively) ($p = 5.06 \times 10^{-7}$) (Figure 6F). This effect was similar in 2.5% and 5% low-protein groups (Figures 6G and 6H). Therefore, the low-protein groups did not increase food intake to the level of caloric restricted mice (pair-fed group) when the diet was changed to 20% protein.

Rapamycin blocked the hyperphagia effect of caloric restriction

Mice fed low-protein diets, independent of the dietary fat content, had reduced body fat, low leptin levels, an intact leptin signaling system, and elevated hunger signaling in the brain. Yet they ate less food and did not show hyperphagia when released from the dietary manipulation. Since the hypothalamic mTOR signaling pathway was also extensively modified by the

(D–H) Average 24-h food intake of 1%, 2.5%, and 5% protein group and 20% protein pair feeding group before and after *ad libitum* fed the 20% protein diet and food intake of 20% protein group ($n = 8$).

(I) The energy expenditure changes of 1% protein and 20% protein pair feeding group.

(J–Q) Hypothalamic p-S6K1 expression levels in (J and K) 1% protein and 20% protein pair feeding group ($n = 3$), (L and M) 1% protein and 20% protein group ($n = 3$), and (P and Q) 1% protein and 20% protein pair feeding group after intracerebral injection of DMSO and rapamycin ($n = 3$).

(N and O) Body weight and food intake changes before surgery, after surgery, and after *ad libitum* fed with 20% protein diet ($n = 7$ –10).

(R) Changes of average 24-h food intake of 1% protein DMSO injected group and 20% protein pair feeding DMSO and rapamycin injected group after *ad libitum* fed the 20% protein diet ($n = 7$ –10). Student's *t* test was performed for statistical analysis and differences with $p < 0.05$ were considered to be significant. * $p < 0.05$, ** $p < 0.01$, *** $p < 0.001$, ns $p > 0.05$. Values are represented as mean \pm SD.

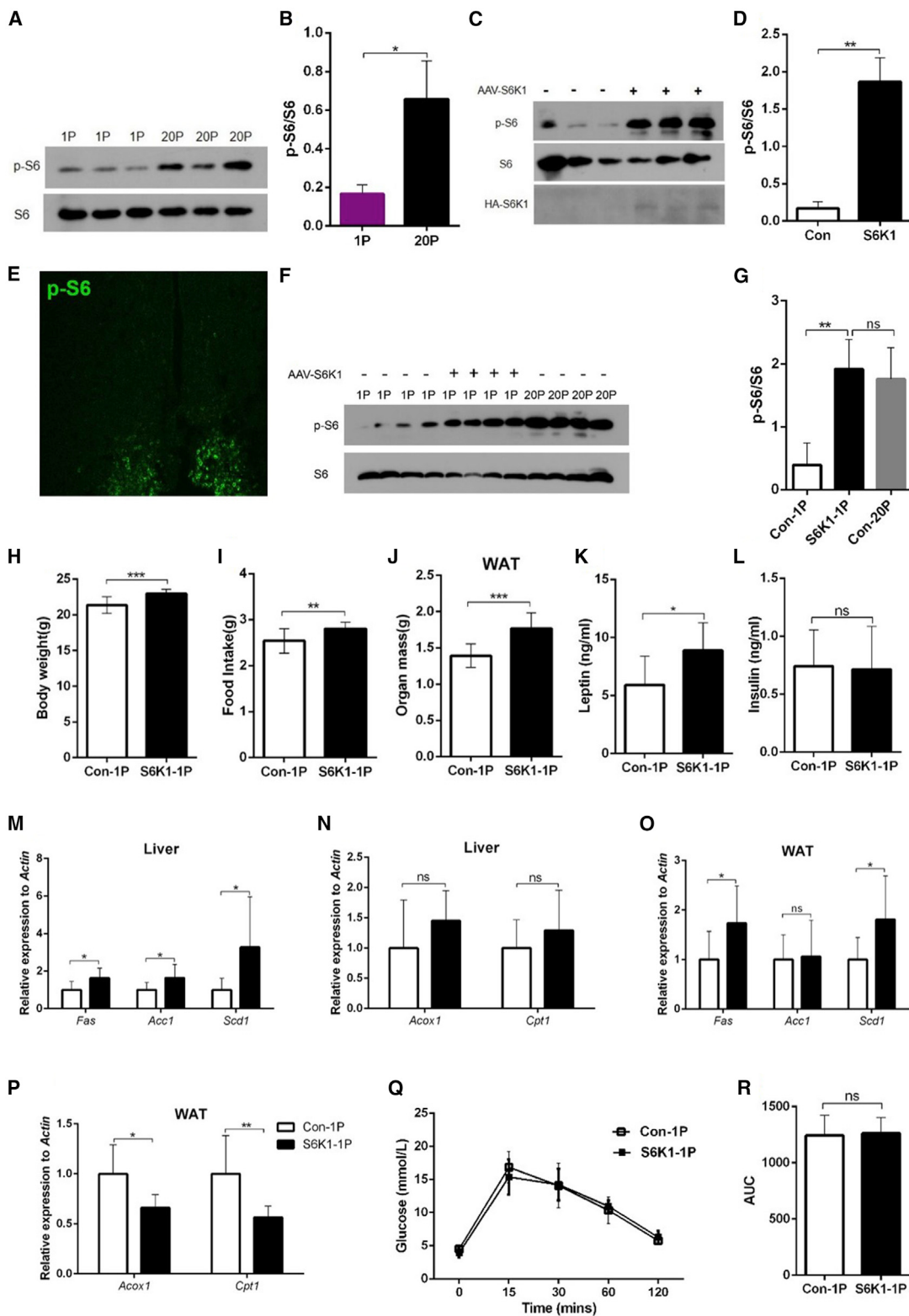


Figure 7. Reduced food intake and body weight of the 1% protein diet is partially dependent on the mTOR signaling pathway

(A–G) Hypothalamic p-S6 protein expression levels in (A and B) 1% protein and 20% protein group, (C and D) control and S6K1 overexpressing AAV injection group ($n = 3$), (F and G) control and S6K1 overexpressing AAV injection group, and control AAV injection group treated with the 20% protein diet ($n = 4$). (E) Immunostaining result of the p-S6 protein in ARC sections of AAV-S6K1 injected mice.

(legend continued on next page)

low-protein levels, we hypothesized that this pathway may act downstream of the canonical hunger signaling pathways to prevent food intake increases.

We compared the hypothalamic p-S6K1 expression level in 1% protein and 20% pair-fed group from the above experiment. We found p-S6K1 had significantly higher expression in 20% pair-fed group compared with the 1% protein group ($p = 0.017$) (Figures 6J and 6K). We also measured the hypothalamic p-S6K1 expression level in 1% protein and 20% protein groups and found the p-S6K1 expression level was significantly decreased in 1% protein group compared with the 20% protein group ($p = 0.005$) (Figures 6L and 6M). To test whether inhibition of hypothalamic p-S6K1 expression could block the hyperphagia effect in the 20% pair feeding group, we fed one group of mice the 1% protein 60% fat diet, and two other groups were pair-fed with 1% protein group using the 20% protein 60% fat diet for 2 weeks. Then one of the 20% pair-fed groups was ICV injected with rapamycin, while the other 20% pair feeding group was ICV injected with vehicle (DMSO). After 1 week of recovery, we provided all treatment groups with *ad libitum* 20% protein 60% fat diet and observed the 24-h food intake (Figures 6N and 6O). Rapamycin treatment significantly inhibited the hypothalamic p-S6K1 expression level ($p = 0.044$ compared with the DMSO treatment group) to almost the same extent as the 1% protein diet, and no significant difference existed in p-S6K1 expression between these two groups ($p > 0.05$) (Figures 6P and 6Q). Moreover, the rapamycin-treated pair-fed group had significantly reduced the food intake compared with the control DMSO-treated group ($p < 0.001$), in the 24 h *ad libitum* conditions, with the food intake decreased to a level not significantly different from the 1% protein group ($p > 0.05$) (Figures 6R). These data suggest that mice fed 1% protein did not elevate their food intake because the low protein in the diet inhibited mTOR signaling, which then acted downstream of the stimulated canonical hunger signaling pathway to block elevated intake.

Reduced food intake, body weight, and fatty acid metabolism changes of the 1% protein diet were partially dependent on the mTOR signaling pathway

The low-protein groups had significantly decreased p-S6K1 and p-S6 expressions compared with the 20% protein group both in hypothalamus and liver ($p < 0.05$) (Figures 7A, 7B, and S6A–S6H). To further explore whether the low food intake of the 1% dietary protein group could be modulated by hypothalamic activation of the mTOR pathway alone, we ICV injected S6K1 overexpressing adeno-associated virus (AAV-S6K1) to activate the mTOR signaling pathway in the hypothalamus. Compared with a control AAV-expressing green fluorescent protein (GFP), hypothalamic p-S6 expression of the S6K1 overexpressing AAV injection group was significantly activated ($p = 0.001$) (Figures 7C–7E). There was no significant p-S6 expression difference between the AAV-S6K1 injection 1% protein group and the control AAV injection 20% protein treatment group

($p > 0.05$) (Figures 7F and 7G). Also, the expression of p-S6 in the liver was not significantly different between the two groups (Figures S6I and S6J). Once the AAV became active (Figures 7C and 7D), the mice were fed the 1% protein diet. The body weight of both S6K1 and control AAV injection treatment groups decreased after feeding on the 1% protein diet, but the body weight of AAV-S6K1 injection group decreased significantly less than those injected with the control virus ($p < 0.001$). After 2 weeks of dietary exposure, the AAV-S6K1 injection group had significantly higher body weight compared with the control virus injection group ($p < 0.001$) (Figure 7H). Moreover, the food intake was significantly higher than the control group ($p = 0.005$) (Figure 7I). After dissection, we found the white adipose tissue weight was also significantly higher in AAV-S6K1 injection group ($p = 0.0004$) (Figure 7J). Leptin but not insulin levels were significantly increased in the AAV-S6K1 injection group ($p = 0.041$) after treatment with the 1% protein diet (Figures 7K and 7L). Further, the fatty acid synthesis genes *Fas*, *Acc1*, and *Scd1* were all significantly upregulated in liver in AAV-S6K1 injection group compared with the control group ($p = 0.038$, $p = 0.039$, $p = 0.048$), but there were no significant differences for fatty acid oxidation genes *Acox1* and *Cpt1* ($p > 0.05$) (Figures 7M and 7N). In white adipose tissue, the fatty acid synthesis genes, *Fas* and *Scd1*, were also significantly upregulated by the AAV-S6K1 treatment ($p = 0.042$, $p = 0.041$, $p = 0.042$, respectively) (Figure 7O). However, in the AAV-S6K1 injection group, the fatty acid oxidation genes, *Acox1* and *Cpt1*, were significantly decreased compared with the control group ($p = 0.014$, $p = 0.008$) (Figure 7P). There was no significant AUC difference in the ipGTT between the control and AAV-S6K1 injection group after they were fed the 1% protein diet ($p > 0.05$) (Figures 7Q and 7R). In summary, the body weight, food intake, serum leptin, and fatty acid metabolism changes induced by 1% protein diet were partially reversed by the hypothalamic activation of mTOR signaling.

1% protein-induced weight loss was not dependent on the hypothalamic GCN2, FGF21, TRPML1, and NTS mTOR signaling

A recent study showed that rapamycin can induce apoptosis via a novel target: transient receptor potential mucolipin 1 (TRPML1) independent of the mTOR pathway (Zhang et al., 2019). It has also been indicated in previous studies that *elf2a* and *Fgf21* signaling pathways were related to the protein-restriction-induced body weight and food-intake changes (Hill et al., 2019; Maurin et al., 2014). To establish whether these genes were involved in the regulation of body weight and food-intake changes in the 1% protein group, we measured hypothalamic gene-expression patterns in 1% protein and 20% protein groups, respectively. We found that *TRPML1*, *p-eIF2a*, and *βklotho* (*Fgf21* receptor) were all significantly increased in 1% protein group ($p = 0.014$, $p = 0.023$, $p = 0.031$, respectively) (Figures S7A–S7C). We ICV injected mice with AAVs expressing control,

(H–R) (H–J) Average body weight changes on last day of measurement, average food intake changes of entire treatment period, average white adipose tissue weight ($n = 10\text{--}13$), (K and L) serum leptin and insulin concentration ($n = 7$), (M–P) relative mRNA expressions of fatty acid metabolism-related genes to *β-actin* ($n = 6\text{--}9$), and (Q and R) the result of glucose tolerance test ($n = 8$) of control and S6K1 overexpressing AAV injection group after treated with 1% protein diet, respectively. Student's *t* test was performed for statistical analysis and differences with $p < 0.05$ were considered to be significant. * $p < 0.05$, ** $p < 0.01$, *** $p < 0.001$, ns $p > 0.05$. Values are represented as mean \pm SD. See also Figure S8.

TRPML1, GCN2, and β klotho shRNA to block the expression of these genes (Figures S7D–S7G). After exposure to the 1% protein diet, there was no significant difference between control and AAV injection groups for body weight and food-intake changes ($p > 0.05$) (Figures S7H–S7M), indicating the impact of the diet on these genes was not the primary mechanism causing the altered food intake and body weight. It has also been shown that the nucleus of the solitary tract (NTS) in the brainstem regulates food intake and body weight through the activation of the S6K1 pathway (Blouet and Schwartz, 2012). Therefore, we also ICV injected control and AAV-S6K1 to the NTS, followed by treatment with the 1% protein diet (Figures S7N and S7O). We found no significant body weight and food-intake differences between NTS control and AAV-S6K1 injection groups ($p > 0.05$) (Figures S7P–S7Q). In summary, reduced food intake of the 1% protein group was partially restored by activation of the hypothalamic mTOR signaling pathway, but not by activation of mTOR in the NTS, and not by reduced p-eIF2a, β klotho, and TRPML1 expression in the hypothalamus.

Results overview

Very low-protein diets (1% and 2.5% protein) independent of dietary fat content, resulted in a dramatic loss of body weight and body fat. This fat loss led to reduced levels of leptin, and stimulation of the canonical hypothalamic hunger signaling pathway. Yet the mice had reduced food intake and showed no hyperphagia when released to feed on diets with 20% protein. Leptin signaling was shown to be intact by injecting exogenous leptin. RNA-seq analysis indicated inhibition of the hypothalamic mTOR pathway, and we also found modulated phosphorylation of S6K1, the downstream target of mTOR. Using a combination of ICV treatment with rapamycin and AAV-S6K1, we showed that very-low-protein diets have reduced food intake, despite reduced circulating leptin and stimulated hunger pathways because inhibition of mTOR acts downstream of these pathways in the hypothalamus to block elevated intake. In contrast, inhibition of eIF2a, TRPML1, and Fgf21 signaling pathways was not related to the low-protein-induced weight loss.

DISCUSSION

Previous work suggested dietary protein levels regulate energy intake because animals eat primarily to satisfy their protein needs. Hence, when dietary protein declines, food and energy intake is predicted to increase: the protein leverage hypothesis (Simpson and Raubenheimer, 2012). This may potentially explain excess caloric consumption and obesity (Huang et al., 2013). We previously explored the impacts of variable dietary protein levels (5% to 30%) in 5 strains of mice (Hu et al., 2018) but did not find significantly stimulated intake at lower protein levels. This contrasted with another large dietary matrix study, which suggested reduced protein was related to stimulated intake (Solon-Biet et al., 2014), and several other smaller studies that have compared low protein to standard protein (20%) diets (Laeger et al., 2016, 2014).

There are several potential reasons for the different results. The age of onset and the makeup of the other dietary components was different between studies. However, the difference could be only a matter of degree of protein content because

with the lowest protein diet we did find a small increase in food intake (although not in fat storage). In part then the motivation for the current experiments was to see if a protein leverage effect would become apparent at dietary protein levels below 5%. We found completely the opposite. At these very-low-protein levels, dietary intake was not stimulated but strongly inhibited, and in consequence, even when the diet contained 60% fat, the mice had substantially lower body weight. Decreased body weight resulted from significant decreases in weights of all the adipose tissues, the liver, and reproductive organs. This preferential utilization of fat tissues was similar to that observed in mice under enforced caloric restriction (CR) at high (20%) protein levels (Mitchell et al., 2015b). The main differences were that under CR the liver was also protected and the alimentary tract actually grew in size (Mitchell et al., 2015b). Similar to the changes under CR, the reduction in the size of the adipose tissue was mostly due to hypotrophy rather than hypoplasia. However, the number of white adipose cells may have also decreased as the percent decrease of WAT weight was larger than the percent decrease in cell volume. Hence, at very-low-protein levels the food intake and body composition changes of the mice responded similarly to mice under CR, but in strong contrast to mice under CR, they had *ad libitum* access to food that they chose not to consume.

The fatty acid metabolism in liver and WAT was greatly changed in low-protein groups. Fatty acid oxidation genes were upregulated in both tissues but fatty acid synthesis genes were only downregulated in the liver and remained unchanged in the WAT. The gene-expression patterns in the liver in the present study were similar to those in previous studies of leucine and methionine restriction (Anthony et al., 2013; Cheng et al., 2010; Orgeron et al., 2014). However, the white adipose lipogenic gene-expression levels were different. In the methionine-restricted mice, lipogenic genes were increased, whereas during leucine deprivation, the lipogenic genes were downregulated (Cheng et al., 2010; Orgeron et al., 2014).

The low-protein sensing pathway already described in many studies (Guo and Cavener, 2007; Laeger et al., 2016, 2014) was also altered in our study, indicated by the higher mRNA levels of ATF4 and *Fgf21* and increased protein level of p-eIF2a in the low-protein groups. FGF21 was also recently emphasized as an indicator of and mediator of the metabolic benefits of protein restriction in mice (Laeger et al., 2014). We also found that the *Fgf21* mRNA level was increased in the liver in low-protein groups. The *Fgf21* expression level was significantly related to the AUC in the ipGTT ($p < 0.001$) independent of the body weight (multiple regression: $p < 0.001$).

The hypothalamus is the main brain region controlling energy balance. We found that the canonical hunger signaling pathway was significantly upregulated in the hypothalamus, but there were no significant changes for dopamine, serotonin, and opioid receptor expression levels. These changes also mirror the hypothalamic gene-expression changes observed in mice under CR (Derous et al., 2016a, 2016b; Hambly et al., 2007). In particular, there was, in both situations, a stimulation of *Npy* and *AgRP* levels and a reduction in *Pomc* and *Cart*. This suggested that in both situations the mice were hungry. When mice under CR are released from restriction these changes lead to post restriction hyperphagia (Hambly et al., 2007). We have shown previously that this hyperphagia is partly driven by the reduced circulating

leptin levels (Hambly et al., 2007) that accompany fat loss under CR (Mitchell et al., 2015a). At very low dietary protein levels we found a similar pattern of response—fat loss was increased, leptin levels were reduced, and the hypothalamic signaling pathway was stimulated. Despite these changes, the mice did not increase consumption of the protein-restricted diet, even though it was available in excess, and they did not show hyperphagia when changed from the 1% to a 20% protein diet.

This suggested something downstream of the canonical hunger pathway in the hypothalamus was interfering with the translation of these changes into altered feeding behavior. A key difference in the RNA-seq responses of mice under CR (Derous et al., 2016a, 2016b) and those observed here was that, at low-protein levels, there was strong inhibition of mTOR signaling. Previous work implicated mTOR signaling in the regulation of food intake (Cota et al., 2006; Dagon et al., 2012; Varela et al., 2012), hence this was a strong candidate explaining the different responses. We showed that in mice under CR (pair-fed to the 1% protein diet) that ICV injection with rapamycin, an inhibitor of mTOR, also blunted the hyperphagic post-restriction response. Previous work in rats that have shown peripheral injection of rapamycin also blocks post-restriction hyperphagia (Kenny et al., 2019). The mTOR signaling pathway changes in the 1% protein group were the same as observed under leucine deprivation (Xia et al., 2012) where it was shown that the impacts of leucine deprivation on energy expenditure and weight loss were completely blocked by the central activation of mTOR.

Several studies investigated the role of mTOR in different tissues other than the central nervous system. One study indicated that mothers fed a low-protein diet during the last week of pregnancy activated mTORC signaling in the β cell in offspring (Alessandro et al., 2014). In addition, l-lysine administration increased mTOR signaling in the skeletal muscle of rats fed a low-protein diet (Sato et al., 2015). Furthermore, it was shown that leucine deprivation-induced insulin sensitivity was dependent on the hepatic mTOR pathway (Xiao et al., 2011). BCAAs also caused hepatic mTOR activation and induced hepatic lipotoxicity (Zhang et al., 2016). In contrast, other studies reported that a low-protein diet (5.77% protein) ameliorated diabetic nephropathy by suppression of mTORC1 activity in the kidney in Wistar fatty rats (Kitada et al., 2016, 2019). In the most recent study, it has been indicated that high protein diets caused increased cardiovascular risk by increasing the macrophage mTOR signal (Zhang et al., 2020). However, no previous studies investigated the hypothalamic mTOR signaling effects on metabolic regulation under protein restriction. Therefore, novel here is the elucidation of the role of the hypothalamic mTOR signaling pathway in mediating the impact of very-low-protein diets on energy balance. We found there were significant differences in body weight, food intake, and fatty acid metabolism between control and AAV-S6K1 injection group after feeding on the 1% protein diet, whereas the glucose tolerance ability was not different in these two groups. In contrast, a previous study indicated that S6K1 in the Pomp and AgRP neurons regulates glucose homeostasis but not the feeding (Smith et al., 2015). There are several potential reasons for the difference between the studies. The major difference may be related to the diet, we explored the role of hypothalamic S6K1 on energy balance and glucose homeostasis under the

low-protein condition, whereas the standard and high-fat diet were used in the previous study. Second, the AAV-S6K1 was expressed in the whole ARC nucleus, which included many neuron cell types in addition to the Pomp and AgRP neurons manipulated in the previous study.

It has recently been shown that rapamycin not only inhibits mTOR but has other mTOR independent effects via TRPML1 (Zhang et al., 2019). It was possible therefore that the impact of rapamycin on post-restriction hyperphagia was unrelated to its impact on mTOR but via the TRPML1 pathway. We also found the eIF2a signaling pathway was the most affected pathway related to the dietary protein content, and recent studies showed that amino-acid-restriction-induced weight loss was dependent on the hypothalamic overexpression of p-eIF2a (Maurin et al., 2014). Moreover, some studies revealed Fgf21 is involved in the regulation of protein restriction impact on energy balance. For example, Fgf21 is required for metabolic responses to protein restriction (Laeger et al., 2014), and deletion of FGF21 co-receptor β klotho from the brain stopped mice responding to a protein-restricted diet (Hill et al., 2019). Energy balance is mainly regulated by signaling molecules in the hypothalamus in the central nervous system. However, neurons sensitive to energy-related signals are also located outside the hypothalamus, for example, the NTS, in the brainstem, regulates food intake and body weight through the activation of the S6K1 pathway (Blouet and Schwartz, 2012). Despite this, we found no significant body weight and food-intake changes in the AAV-GCN2-shRNA, AAV-TRPML1-shRNA, AAV- β klotho-shRNA, and NTS AAV-S6K1 injection groups compared with the control AAV injection group after exposure to the 1% low-protein diet. We demonstrated this was not the case using AAV to stimulate S6K1 in NTS or inhibit TRPML1, GCN2, or β klotho and showed only the stimulation of S6K1 in hypothalamus modulated the protein restriction effect.

Conclusion and implications

Extremely low levels of dietary protein led mice to reduce their food intake with consequent changes in body composition (largely comprising loss of body fat). These effects occurred despite *ad libitum* access to food and despite their reduced body fat leading to lowered leptin levels and stimulation of the canonical hypothalamic hunger pathway including stimulated *Npy* and *AgRP* and reduced *Pomp* and *Cart*. Moreover, contrasting mice under CR, these mice did not show hyperphagia when released from their dietary constraint. Low dietary protein also inhibited hypothalamic mTOR signaling and we showed that this inhibition is integral to their lack of hunger response. It is unclear at present if these pathways are conserved in humans. If they are, this raises the interesting possibility of using rapamycin (or other mTOR inhibitors) as an adjunct therapy to CR in humans that are aiming to reduce body weight. This would blunt the resultant stimulation of hunger, which is seen as a key driver for people to break their calorie-restricted diets. Our work suggests that combining restriction with very low protein may potentially generate similar effects.

Limitations of study

There were several limitations to this study. We performed experiments on a single mouse strain (C57BL/6N) and single sex (male). Although our previous work indicated that different

mouse strains had similar responses to different macronutrient composition diets (Hu et al., 2018) the translational relevance of the work would be improved if it was repeated in other strains of mice and ideally non-human primates. We found that injection of AAV-S6K1 influenced the energy regulation of the mice, but we did not measure the levels of the main hunger signaling genes in this condition. This requires further work to elucidate where the action of the mTOR signaling pathway interacts with the canonical hunger signaling system. Finally, we only used a single type of protein (Casein) in the diet. Previous studies have indicated that protein source had a significant effect on body fat (McManus et al., 2015). Thus, the impact of low protein may be mediated via the effects of one or a few individual amino acids. Further work should explore the potential roles that different amino acids and different sources of protein may play in these effects.

STAR★METHODS

Detailed methods are provided in the online version of this paper and include the following:

- **KEY RESOURCES TABLE**
- **RESOURCE AVAILABILITY**
 - Lead contact
 - Materials availability
- **DATA AND CODE AVAILABILITY**
- **EXPERIMENTAL MODEL AND SUBJECT DETAILS**
 - Ethical Statement
 - Mice
- **METHOD DETAILS**
 - Experimental diets
 - Metabolic phenotype measurement
 - Glucose tolerance test and leptin sensitivity test
 - Performance assays
 - Hormone measurements
 - Quantitative RT-PCR
 - Western blotting
 - In situ hybridization
 - Immunostaining
 - Histology
 - Transcriptome data analysis
 - Metabolomics measurement and analysis
 - Pair feeding experiment
 - Intracerebral rapamycin infusion
 - Intracerebral virus injection
- **QUANTIFICATION AND STATISTICAL ANALYSIS**

SUPPLEMENTAL INFORMATION

Supplemental information can be found online at <https://doi.org/10.1016/j.cmet.2021.01.017>.

ACKNOWLEDGMENTS

The study was funded by the National Key R&D Program of China (2019YFA0801900), Chinese Academy of Sciences Strategic Program (XDB13030100), the National Natural Science Foundation of China (31570409), the 1000 Talents program, a PIFI professorial fellowship award, the KC Wong Foundation, and a Wolfson merit award to J.R.S.

AUTHOR CONTRIBUTIONS

J.R.S. directed the project, conceived and designed the experiments, contributed to the analysis, and co-wrote the paper. Y.W. conducted the experiments, analyzed the data, and co-wrote the manuscript. B.L., L.L., S.E.M., G.W., L.W., M.L., J.L., C.N., Z.J., A.W., and Y.Z. contributed to the data collection. A.D. and C.L.G. contributed to RNA-seq, metabolomics raw data, and IPA-related analysis. All authors approved the final version prior to submission for publication.

DECLARATION OF INTERESTS

The authors declare no competing interests.

Received: March 13, 2020

Revised: October 5, 2020

Accepted: January 21, 2021

Published: March 4, 2021

REFERENCES

- Ahima, R.S., and Antwi, D.A. (2008). Brain regulation of appetite and satiety. *Endocrinol. Metab. Clin. North Am.* **37**, 811–823.
- Akhan, I., Sayar Atasoy, N., Yavuz, Y., Ates, T., Coban, I., Koksalar, F., Filiz, G., Topcu, I.C., Oncul, M., Dilsiz, P., et al. (2020). NTS catecholamine neurons mediate hypoglycemic hunger via medial hypothalamic feeding pathways. *Cell Metab.* **31**, 313–326.e5.
- Alejandro, E.U., Gregg, B., Wallen, T., Kumusoglu, D., Meister, D., Chen, A., Merrins, M.J., Satin, L.S., Liu, M., Arvan, P., and Bernal-Mizrachi, E. (2014). Maternal diet-induced microRNAs and mTOR underlie β cell dysfunction in offspring. *J. Clin. Invest.* **124**, 4395–4410.
- Anders, S., McCarthy, D.J., Chen, Y., Okoniewski, M., Smyth, G.K., Huber, W., and Robinson, M.D. (2013). Count-based differential expression analysis of RNA sequencing data using R and Bioconductor. *Nat. Protoc.* **8**, 1765–1786.
- Andrikopoulos, S., Blair, A.R., Deluca, N., Fam, B.C., and Proietto, J. (2008). Evaluating the glucose tolerance test in mice. *Am. J. Physiol. Endocrinol. Metab.* **295**, E1323–E1332.
- Anthony, T.G., Morrison, C.D., and Gettys, T.W. (2013). Remodeling of lipid metabolism by dietary restriction of essential amino acids. *Diabetes* **62**, 2635–2644.
- Beugnet, A., Tee, A.R., Taylor, P.M., and Proud, C.G. (2003). Regulation of targets of mTOR (mammalian target of rapamycin) signalling by intracellular amino acid availability. *Biochem. J.* **372**, 555–566.
- Blouet, C., and Schwartz, G.J. (2012). Brainstem nutrient sensing in the nucleus of the solitary tract inhibits feeding. *Cell Metab.* **16**, 579–587.
- Carroll, B., Maetzel, D., Maddocks, O.D., Otten, G., Ratcliff, M., Smith, G.R., Dunlop, E.A., Passos, J.F., Davies, O.R., Jaenisch, R., et al. (2016). Control of TSC2-Rheb signaling axis by arginine regulates mTORC1 activity. *eLife* **5**, e11058.
- Cheng, Y., Meng, Q., Wang, C., Li, H., Huang, Z., Chen, S., Xiao, F., and Guo, F. (2010). Leucine deprivation decreases fat mass by stimulation of lipolysis in white adipose tissue and upregulation of uncoupling protein 1 (UCP1) in brown adipose tissue. *Diabetes* **59**, 17–25.
- Cota, D., Proulx, K., Smith, K.A., Kozma, S.C., Thomas, G., Woods, S.C., and Seeley, R.J. (2006). Hypothalamic mTOR signaling regulates food intake. *Science* **312**, 927–930.
- Dagon, Y., Hur, E., Zheng, B., Wellenstein, K., Cantley, L.C., and Kahn, B.B. (2012). P70S6 kinase phosphorylates AMPK on serine 491 to mediate leptin's effect on food intake. *Cell Metab.* **16**, 104–112.
- De Livera, A.M., Dias, D.A., De Souza, D., Rupasinghe, T., Pyke, J., Tull, D., Roessner, U., McConville, M., and Speed, T.P. (2012). Normalizing and integrating metabolomics data. *Anal. Chem.* **84**, 10768–10776.
- De Livera, A.M., Olshansky, M., and Speed, T.P. (2013). Statistical analysis of metabolomics data. *Methods Mol. Biol.* **1055**, 291–307.
- Deros, D., Mitchell, S.E., Green, C.L., Chen, L., Han, J.D., Wang, Y., Promislow, D.E., Lusseau, D., Speakman, J.R., and Douglas, A. (2016a). The

- effects of graded levels of calorie restriction: VI. Impact of short-term graded calorie restriction on transcriptomic responses of the hypothalamic hunger and circadian signaling pathways. *Aging* 8, 642–663.
- Derous, D., Mitchell, S.E., Green, C.L., Wang, Y., Han, J.D., Chen, L., Promislow, D.E., Lusseau, D., Speakman, J.R., and Douglas, A. (2016b). The effects of graded levels of calorie restriction: VII. Topological rearrangement of hypothalamic aging networks. *Aging* 8, 917–932.
- Fontana, L., Cummings, N.E., Arriola Apelo, S.I., Neuman, J.C., Kasza, I., Schmidt, B.A., Cava, E., Spelta, F., Tostì, V., Syed, F.A., et al. (2016). Decreased consumption of branched-chain amino acids improves metabolic health. *Cell Rep.* 16, 520–530.
- Guo, F., and Cavener, D.R. (2007). The GCN2 eIF2alpha kinase regulates fatty-acid homeostasis in the liver during deprivation of an essential amino acid. *Cell Metab.* 5, 103–114.
- Hambly, C., Simpson, C.A., McIntosh, S., Duncan, J.S., Dalgleish, G.D., and Speakman, J.R. (2007). Calorie-restricted mice that gorge show less ability to compensate for reduced energy intake. *Physiol. Behav.* 92, 985–992.
- Heikkinen, S., Argmann, C.A., Champy, M.F., and Auwerx, J. (2007). Evaluation of glucose homeostasis. *Curr. Protoc. Mol. Biol.* 77, 29B.3.1–29B.3.22.
- Hill, C.M., Laeger, T., Dehner, M., Albarado, D.C., Clarke, B., Wanders, D., Burke, S.J., Collier, J.J., Qualls-Creekmore, E., Solon-Biet, S.M., et al. (2019). FGF21 signals protein status to the brain and adaptively regulates food choice and metabolism. *Cell Rep.* 27, 2934–2947.e3.
- Hu, S., Wang, L., Yang, D., Li, L., Togo, J., Wu, Y., Liu, Q., Li, B., Li, M., Wang, G., et al. (2018). Dietary fat, but not protein or carbohydrate, regulates energy intake and causes adiposity in mice. *Cell Metab.* 28, 415–431.e4.
- Huang, X., Hancock, D.P., Gosby, A.K., McMahon, A.C., Solon, S.M., Le Couteur, D.G., Conigrave, A.D., Raubenheimer, D., and Simpson, S.J. (2013). Effects of dietary protein to carbohydrate balance on energy intake, fat storage, and heat production in mice. *Obesity (Silver Spring)* 21, 85–92.
- Jewell, J.L., Kim, Y.C., Russell, R.C., Yu, F.X., Park, H.W., Plouffe, S.W., Tagliabracci, V.S., and Guan, K.L. (2015). Metabolism. Differential regulation of mTORC1 by leucine and glutamine. *Science* 347, 194–198.
- Keller, U. (2011). Dietary proteins in obesity and in diabetes. *Int. J. Vitam. Nutr. Res.* 81, 125–133.
- Kenny, T.E., Hebert, M., MacCallum, P., Whiteman, J., Martin, G.M., and Blundell, J. (2019). Single injection of rapamycin blocks post-food restriction hyperphagia and body-weight regain in rats. *Behav. Neurosci.* 133, 98–109.
- Kim, D., Langmead, B., and Salzberg, S.L. (2015). HISAT: a fast spliced aligner with low memory requirements. *Nat. Methods* 12, 357–360.
- Kitada, M., Ogura, Y., Monno, I., and Koya, D. (2019). The impact of dietary protein intake on longevity and metabolic health. *EBioMedicine* 43, 632–640.
- Kitada, M., Ogura, Y., Suzuki, T., Sen, S., Lee, S.M., Kanasaki, K., Kume, S., and Koya, D. (2016). A very-low-protein diet ameliorates advanced diabetic nephropathy through autophagy induction by suppression of mTORC1 pathway in Wistar fatty rats, an animal model of type 2 diabetes and obesity. *Diabetologia* 59, 1307–1317.
- Kleinridders, A., Schenten, D., Konner, A.C., Belgardt, B.F., Mauer, J., Okamura, T., Wunderlich, F.T., Medzhitov, R., and Brüning, J.C. (2009). MyD88 signaling in the CNS is required for development of fatty acid-induced leptin resistance and diet-induced obesity. *Cell Metab.* 10, 249–259.
- Laeger, T., Albarado, D.C., Burke, S.J., Trosclair, L., Hedgepeth, J.W., Berthoud, H.R., Gettys, T.W., Collier, J.J., Münzberg, H., and Morrison, C.D. (2016). Metabolic responses to dietary protein restriction require an increase in FGF21 that is delayed by the absence of GCN2. *Cell Rep.* 16, 707–716.
- Laeger, T., Henagan, T.M., Albarado, D.C., Redman, L.M., Bray, G.A., Noland, R.C., Münzberg, H., Hutson, S.M., Gettys, T.W., Schwartz, M.W., and Morrison, C.D. (2014). FGF21 is an endocrine signal of protein restriction. *J. Clin. Invest.* 124, 3913–3922.
- Li, H., Handsaker, B., Wysoker, A., Fennell, T., Ruan, J., Homer, N., Marth, G., Abecasis, G., and Durbin, R.; 1000 Genome Project Data Processing Subgroup (2009). The sequence alignment/Map format and SAMtools. *Bioinformatics* 25, 2078–2079.
- Liao, Y., Smyth, G.K., and Shi, W. (2013). The subread aligner: fast, accurate and scalable read mapping by seed-and-vote. *Nucleic Acids Res.* 41, e108.
- Liao, Y., Smyth, G.K., and Shi, W. (2014). featureCounts: an efficient general purpose program for assigning sequence reads to genomic features. *Bioinformatics* 30, 923–930.
- Lund, S.P., Nettleton, D., McCarthy, D.J., and Smyth, G.K. (2012). Detecting differential expression in RNA-sequence data using quasi-likelihood with shrunken dispersion estimates. *Stat. Appl. Genet. Mol. Biol.* 11.
- Maurin, A.C., Benani, A., Lorsignol, A., Brenachot, X., Parry, L., Carraro, V., Guissard, C., Averous, J., Jousse, C., Bruhat, A., et al. (2014). Hypothalamic eIF2alpha signaling regulates food intake. *Cell Rep.* 6, 438–444.
- McCarthy, D.J., Chen, Y., and Smyth, G.K. (2012). Differential expression analysis of multifactor RNA-seq experiments with respect to biological variation. *Nucleic Acids Res.* 40, 4288–4297.
- McGuinness, O.P., Ayala, J.E., Laughlin, M.R., and Wasserman, D.H. (2009). NIH experiment in centralized mouse phenotyping: the Vanderbilt experience and recommendations for evaluating glucose homeostasis in the mouse. *Am. J. Physiol. Endocrinol. Metab.* 297, E849–E855.
- McManus, B.L., Korpela, R., Speakman, J.R., Cryan, J.F., Cotter, P.D., and Nilaweera, K.N. (2015). Bovine serum albumin as the dominant form of dietary protein reduces subcutaneous fat mass, plasma leptin and plasma corticosterone in high fat-fed C57/BL6 mice. *Br. J. Nutr.* 114, 654–662.
- Mitchell, S.E., Delville, C., Konstantopoulos, P., Hurst, J., Derous, D., Green, C., Chen, L., Han, J.J., Wang, Y., Promislow, D.E., et al. (2015a). The effects of graded levels of calorie restriction: II. Impact of short term calorie and protein restriction on circulating hormone levels, glucose homeostasis and oxidative stress in male C57BL/6 mice. *Oncotarget* 6, 23213–23237.
- Mitchell, S.E., Tang, Z., Kerbois, C., Delville, C., Konstantopoulos, P., Bruel, A., Derous, D., Green, C., Aspden, R.M., Goodyear, S.R., et al. (2015b). The effects of graded levels of calorie restriction: I. impact of short term calorie and protein restriction on body composition in the C57BL/6 mouse. *Oncotarget* 6, 15902–15930.
- Muniyappa, R., Lee, S., Chen, H., and Quon, M.J. (2008). Current approaches for assessing insulin sensitivity and resistance in vivo: advantages, limitations, and appropriate usage. *Am. J. Physiol. Endocrinol. Metab.* 294, E15–E26.
- Nixon, J.P., Zhang, M., Wang, C., Kuskowski, M.A., Novak, C.M., Levine, J.A., Billington, C.J., and Kotz, C.M. (2010). Evaluation of a quantitative magnetic resonance imaging system for whole body composition analysis in rodents. *Obesity (Silver Spring)* 18, 1652–1659.
- Orgeron, M.L., Stone, K.P., Wanders, D., Cortez, C.C., Van, N.T., and Gettys, T.W. (2014). The impact of dietary methionine restriction on biomarkers of metabolic health. *Prog. Mol. Biol. Transl. Sci.* 121, 351–376.
- Pertea, M., Kim, D., Pertea, G.M., Leek, J.T., and Salzberg, S.L. (2016). Transcript-level expression analysis of RNA-seq experiments with HISAT, StringTie and Ballgown. *Nat. Protoc.* 11, 1650–1667.
- R Core Team (2015). R: a language and environment for statistical computing (R Foundation for Statistical Computing). <https://www.R-project.org/>.
- Robinson, M.D., McCarthy, D.J., and Smyth, G.K. (2010). edgeR: a Bioconductor package for differential expression analysis of digital gene expression data. *Bioinformatics* 26, 139–140.
- Robinson, M.D., and Oshlack, A. (2010). A scaling normalization method for differential expression analysis of RNA-seq data. *Genome Biol.* 11, R25.
- Robinson, M.D., and Smyth, G.K. (2007). Moderated statistical tests for assessing differences in tag abundance. *Bioinformatics* 23, 2881–2887.
- Sato, T., Ito, Y., and Nagasawa, T. (2015). Dietary L-lysine suppresses autophagic proteolysis and stimulates Akt/mTOR signaling in the skeletal muscle of rats fed a low-protein diet. *J. Agric. Food Chem.* 63, 8192–8198.
- Schutz, Y. (1995). Macronutrients and energy balance in obesity. *Metabolism* 44, 7–11.
- Schwartz, M.W., Woods, S.C., Porte, D., Jr., Seeley, R.J., and Baskin, D.G. (2000). Central nervous system control of food intake. *Nature* 404, 661–671.
- Simpson, S., and Raubenheimer, D. (2012). The Nature of Nutrition: A Unifying Framework from Animal Adaption to Human Obesity (Princeton University Press).

- Smith, C.A., Want, E.J., O'Maille, G., Abagyan, R., and Siuzdak, G. (2006). XCMS: processing mass spectrometry data for metabolite profiling using nonlinear peak alignment, matching, and identification. *Anal. Chem.* 78, 779–787.
- Smith, M.A., Katsouri, L., Irvine, E.E., Hankir, M.K., Pedroni, S.M., Voshol, P.J., Gordon, M.W., Choudhury, A.I., Woods, A., Vidal-Puig, A., et al. (2015). Ribosomal S6K1 in POMC and AgRP neurons regulates glucose homeostasis but not feeding behavior in mice. *Cell Rep.* 11, 335–343.
- Solon-Biet, S.M., McMahon, A.C., Ballard, J.W., Ruohonen, K., Wu, L.E., Cogger, V.C., Warren, A., Huang, X., Pichaud, N., Melvin, R.G., et al. (2014). The ratio of macronutrients, not caloric intake, dictates cardiometabolic health, aging, and longevity in ad libitum-fed mice. *Cell Metab.* 19, 418–430.
- Somerville, J.M., Aspden, R.M., Armour, K.E., Armour, K.J., and Reid, D.M. (2004). Growth of C57BL/6 mice and the material and mechanical properties of cortical bone from the tibia. *Calcif. Tissue Int.* 74, 469–475.
- Stekhoven, D.J., and Bühlmann, P. (2012). MissForest—non-parametric missing value imputation for mixed-type data. *Bioinformatics* 28, 112–118.
- Sysi-Aho, M., Katajamaa, M., Yetukuri, L., and Oresic, M. (2007). Normalization method for metabolomics data using optimal selection of multiple internal standards. *BMC Bioinformatics* 8, 93.
- Uppal, K., Walker, D.I., and Jones, D.P. (2017). xMSannotator: an R package for network-based annotation of high-resolution metabolomics data. *Anal. Chem.* 89, 1063–1067.
- Varela, L., Martínez-Sánchez, N., Gallego, R., Vázquez, M.J., Roa, J., Gándara, M., Schoenmakers, E., Nogueiras, R., Chatterjee, K., Tena-Sempere, M., et al. (2012). Hypothalamic mTOR pathway mediates thyroid hormone-induced hyperphagia in hyperthyroidism. *J. Pathol.* 227, 209–222.
- Wang, S., Tsun, Z.Y., Wolfson, R.L., Shen, K., Wyant, G.A., Plovanich, M.E., Yuan, E.D., Jones, T.D., Chantranupong, L., Comb, W., et al. (2015). Metabolism. Lysosomal amino acid transporter SLC38A9 signals arginine sufficiency to mTORC1. *Science* 347, 188–194.
- Weir, J.B. (1949). New methods for calculating metabolic rate with special reference to protein metabolism. *J. Physiol.* 109, 1–9.
- Wilding, J.P. (2002). Neuropeptides and appetite control. *Diabet. Med.* 19, 619–627.
- Xia, T., Cheng, Y., Zhang, Q., Xiao, F., Liu, B., Chen, S., and Guo, F. (2012). S6K1 in the central nervous system regulates energy expenditure via MC4R/CRH pathways in response to deprivation of an essential amino acid. *Diabetes* 61, 2461–2471.
- Xiao, F., Huang, Z., Li, H., Yu, J., Wang, C., Chen, S., Meng, Q., Cheng, Y., Gao, X., Li, J., et al. (2011). Leucine deprivation increases hepatic insulin sensitivity via GCN2/mTOR/S6K1 and AMPK pathways. *Diabetes* 60, 746–756.
- Yang, S.B., Tien, A.C., Boddupalli, G., Xu, A.W., Jan, Y.N., and Jan, L.Y. (2012). Rapamycin ameliorates age-dependent obesity associated with increased mTOR signaling in hypothalamic POMC neurons. *Neuron* 75, 425–436.
- Yang, Y., Zhang, Y., Xu, Y., Luo, T., Ge, Y., Jiang, Y., Shi, Y., Sun, J., and Le, G. (2019). Dietary methionine restriction improves the gut microbiota and reduces intestinal permeability and inflammation in high-fat-fed mice. *Food Funct.* 10, 5952–5968.
- Zhang, Q., Liu, B., Cheng, Y., Meng, Q., Xia, T., Jiang, L., Chen, S., Liu, Y., and Guo, F. (2014). Leptin signaling is required for leucine deprivation-enhanced energy expenditure. *J. Biol. Chem.* 289, 1779–1787.
- Zhang, X., Chen, W., Gao, Q., Yang, J., Yan, X., Zhao, H., Su, L., Yang, M., Gao, C., Yao, Y., et al. (2019). Rapamycin directly activates lysosomal mucolipin TRP channels independent of mTOR. *PLoS Biol.* 17, e3000252.
- Zhang, X., Sergin, I., Evans, T.D., Jeong, S.J., Rodriguez-Velez, A., Kapoor, D., Chen, S., Song, E., Holloway, K.B., Crowley, J.R., et al. (2020). High-protein diets increase cardiovascular risk by activating macrophage mTOR to suppress mitophagy. *Nat Metab* 2, 110–125.
- Zhang, F., Zhao, S., Yan, W., Xia, Y., Chen, X., Wang, W., Zhang, J., Gao, C., Peng, C., Yan, F., et al. (2016). Branched chain amino acids cause liver injury in obese/diabetic mice by promoting adipocyte lipolysis and inhibiting hepatic autophagy. *EBioMedicine* 13, 157–167.

STAR★METHODS

KEY RESOURCES TABLE

REAGENT or RESOURCE	SOURCE	IDENTIFIER
Antibodies		
p70S6 Kinase	CST	Cat# 9202; RRID: AB_331676
Phospho-p70S6 Kinase (Thr389)	CST	Cat# 9205; RRID: AB_330944
S6 Ribosomal Protein	CST	Cat# 2317; RRID: AB_2238583
Phospho-S6 Ribosomal Protein (Ser235/236)	CST	Cat# 4858; RRID: AB_916156
eIF2a	CST	Cat# 9722; RRID: AB_2230924
Phospho-eIF2a (Ser51)	CST	Cat# 3398; RRID: AB_2096481
Stat3	CST	Cat# 9132; RRID: AB_331588
Phospho-stat3	CST	Cat# 9134; RRID: AB_331589
Klotho	Abcam	Cat# Ab98111; RRID: AB_10678894
TRPML1	Alomone	Cat# ACC-081; RRID: AB_10915894
HA-Tag	Easybio	Cat# BE2061,
β-actin	AmeriBiopharma	Cat# AB1015T,
GFP	Abcam	Cat# Ab92456; RRID: AB_10561923
Cy5-AffiniPure Donkey Anti-Rabbit IgG	Jackson	Cat# 711-175-152; RRID: AB_2340607
Cy5-AffiniPure Donkey Anti-Mouse IgG	Jackson	Cat# 715-175-150; RRID: AB_2340819
Bacterial and virus strains		
pHBAAV-CMV-Rps6kb1-HA-T2A-EGFP	Hanbio	N/A
pHBAAV-U6-shTRPML1-CMV-EGFP	Hanbio	N/A
pHBAAV-U6-shGCN2-CMV-EGFP	Hanbio	N/A
pHBAAV-U6-shklotho-CMV-EGFP	Hanbio	N/A
pHBAAV-U6-con-CMV-EGFP	Hanbio	N/A
Chemicals, peptides, and recombinant proteins		
Trizol	Invitrogen	15596018
SYBR Green PCR kit	TransGen Biotech	EP1602
Protease inhibitor cocktail	Sigma	P8340
PMSF	Sigma	P7626
bicinchoninic acid (BCA) protein quantification kit	ThermoFisher	23227
Immobilon-P PVDF membranes	Millipore	ISEQ00010
ECL blotting reagents	GE Healthcare	RPN2232
Murine leptin	Peprotech	450-31-5000
Rapamycin	LC Labs	R-5000
³⁵ S UTP	PerkinElmer	NEG039C001MC
T7 RNA Polymerase	Promega	P2075
rNTP	Promega	P1221
RNasin Ribonuclease Inhibitor	Promega	N2111
RQ1 RNase-free DNase	Promega	M6101
Formamide	Sigma	F9037
Sodium citrate tribasic dehydrate ACS reagent	Sigma	S4641
Dextran Sulfate	Sigma	D8906
Ribonucleic acid	Sigma	R8508

(Continued on next page)

Continued

REAGENT or RESOURCE	SOURCE	IDENTIFIER
DPX Mountant	Sigma	06522
Denhardt's	Sigma	D9905
DL-Dithiothreitol	Sigma	D0632
Diethyl pyrocarbonate	Sigma	D5758
Critical commercial assays		
Mouse Leptin ELISA kit	Crystalchem	90030
Mouse Insulin ELISA kit	Crystalchem	90080
Mouse Leptin ELISA kit	Merk Millipore	EZML-82K
Mouse Insulin ELISA kit	Merk Millipore	EZRMI-13K
Brain infusion kit	Alzet	Kit3
Osmotic pump	Alzet	1004
Chroma Spin-30 DEPC-H ₂ O Columns	Clontech	636087
Deposited data		
RNA-seq data	NCBI GEO	GSE158215
Metabolomics data	Mendeley	https://doi.org/10.17632/h96dcs23rr.1
Experimental models: organisms/strains		
Mouse: C57BL/6N	Charles River	RRID:IMSR_CRL:27
Oligonucleotides		
Primers	Table S5	N/A
Software and algorithms		
Microsoft Excel	N/A	N/A
Minitab 16	N/A	N/A
R Platform	N/A	N/A
IPA	Ingenuity Systems	N/A
GraphPad Prism	N/A	N/A

RESOURCE AVAILABILITY**Lead contact**

Further information and requests for resources and reagents should be directed to and will be fulfilled by the Lead Contact, John R. Speakman (j.speakman@abdn.ac.uk).

Materials availability

There are no restrictions to the availability of all materials mentioned in the manuscript.

DATA AND CODE AVAILABILITY

The accession number for the transcriptome data for **Figures 5** and **S4** reported in this paper is GEO: [GSE158215](https://www.ncbi.nlm.nih.gov/geo/study/?acc=GSE158215). The metabolomics data for **Figure S5** have been deposited to Mendeley Data, and relevant DOI is as follows: <https://doi.org/10.17632/h96dcs23rr.1>.

EXPERIMENTAL MODEL AND SUBJECT DETAILS**Ethical Statement**

All animal procedures were reviewed and approved by the Institute of Genetics and Developmental Biology Chinese Academy of Sciences: approval numbers for the various experiments were AP2016023, AP2016024, AP2016025 and AP2019034.

Mice

Eight weeks old male C57BL/6N mice were purchased from Charles River, Beijing. All mice were acclimated to the environment for 2 weeks before starting the baseline treatment. During the baseline period, all mice were fed with standard diet which contains 10% fat, 20% protein and 70% carbohydrate (D12450B, Research Diets), then allocated to 10 different special diets (detailed as below) and continuously fed these diets for 12 weeks. During the whole experimental period, mice were singly housed under controlled 22–24°C temperature and 12:12 light dark cycle in SPF facility conditions. Mice were killed by rising concentration of

CO₂ for the normal collection of tissues and serum. Tissues were snap frozen in liquid nitrogen and then stored at -80°C. For the mice used in histology and immunostaining the perfusion (paraformaldehyde) method was used.

METHOD DETAILS

Experimental diets

In 10 different diets, the fat content of first five diets were fixed at 60% by energy and protein content ranged from 1% to 20% (1%, 2.5%, 5%, 10% and 20% respectively) by energy (D14121903, D14121904, D14071601, D14071602, D14071604), another 5 kinds of diets contained the same graded levels of protein content as the first 5 diets but fat contents were fixed at 20% by energy (D14121905, D14121906, D14071607, D14071608, D14071610). The energy difference was compensated by carbohydrates including corn starch and maltodextrose. Casein was used as the protein source in all diets. To mimic the typical western diet a mix of cocoa butter, menhaden oil, sunflower oil, palm oil and coconut oil was used as the fat source and was designed to generate a 47.5: 36.8: 15.8 proportion of saturated, mono-unsaturated and polyunsaturated fats and 14.7: 1 proportion of n-6 and n-3 fatty acids, the proportions of different fat compositions didn't change under two different 60% and 20% fat conditions. Sucrose and cellulose were fixed at 5% level by energy and standard vitamins and mineral mix were also added to all diets as well (Hu et al., 2018). The two series were isocaloric within each series. The full details of all diets are shown in Table S3, S4 and can be ordered directly from the manufacturer (research diets, <https://researchdiets.com>) using the diet codes provided.

Metabolic phenotype measurement

For both baseline and different diets manipulation period body weight and food intake were recorded daily. Food intake was calculated by subtracting the food in the food hopper on the second day from the food placed in the food hopper on the first day. If any food fragments were in the bedding these were returned to the hopper before weighing the food. The fat weight and lean weight were measured weekly during different diets treatment period by using the EchoMRI Body Composition Analyzer (Nixon et al., 2010). Feces were collected at the last week of 12 weeks different diets treatment period and dried at 60°C for 7 days, then measured its energy content by using the oxygen bomb calorimeter (Parr, 1281, USA). The oxygen (O₂) consumption (mL/min), carbon dioxide (CO₂) production (mL/min), physical activity (Counts) and respiratory exchange ratio (RER = VCO₂/VO₂) were measured by TSE Phenomaster system after feeding 10 weeks different diets, actual energy expenditure was calculated by using the Weir Equation: EE (KJ/day) = ((3.9 × VO₂ (mL/min)+1.1 × VCO₂(mL/min)) 1440(min)/1000 × 4.184 (Weir, 1949). To investigate which tissues were the most utilized tissues we plotted the logged final body weight against the final organ weight and then fitted into the linear least regression to express the relative utilization of each tissue, according to this description, if the gradient equals to 1 the organ should be utilized the same rate as the body weight, anything greater than 1 is utilized more than body weight and anything between 0 and 1 should be considered protected.

Glucose tolerance test and leptin sensitivity test

Glucose tolerance test was performed at the eighth week of diets manipulation. Mice were fasted for 14 hours prior to analysis. Baseline blood glucose concentration was measured first. Mice were then intraperitoneal (I.P.) injected glucose (2 g/kg of body weight) and blood glucose concentrations at 15, 30, 60 and 120 min after glucose injection (Andrikopoulos et al., 2008) were measured from tail tip blood samples by using OneTouch ultravue™ glucometer (Qiang Sheng, China). The intra-peritoneal glucose tolerance test we used is a popular indicator of metabolic health, in most cases decreased body fat results in improved glucose tolerance, and as expected, low protein groups in this study had significantly improved glucose tolerance even under high-fat condition. There is controversy about how to choose the glucose injection dose for such tests. Many studies, like ours, have dosed with glucose in relation to body weight, but some advocate the dose should be based on lean weight rather than body weight (McGuinness et al., 2009). Yet others suggest the same dose should be injected to all mice independent of body weight as is performed in oral glucose tolerance tests in humans (Heikkinen et al., 2007; Muniyappa et al., 2008). The choice of which path to follow is not straightforward since injecting in relation to fat-free weight assumes only this compartment partakes in glucose disposal, which is known to be incorrect. But injecting in relation to body weight assumes both fat and lean compartments partake equally which is also incorrect. Consistent with many other studies in the present study, we injected glucose according to the body weight of each mouse, hence leaner mice were given a lower glucose dose. This would tend to favor finding an effect of lower body fat on the glucose tolerance as we did. Whether this is an artefact of the dosing protocol remains open for debate.

Leptin response test was performed at the 8th week of special diets exposure. Mice were fasted for 12 hour before leptin or PBS (Phosphate Buffer Solution) administration by intraperitoneally, leptin (3mg/kg) and PBS were administered at 9:00 am, food intake and body weight were measured at 1 and 4 hour post injection of leptin or PBS. Hypothalamus were collected for measurement of gene and protein expression 45 min after leptin or PBS administration (Zhang et al., 2014)

Performance assays

Grip strength was performed by using the digital grip strength measurement equipment, each mice was tested for three times each day for five consecutive days. The rotarod performance test was determined using the Rota Rod (Ugo Basile). Mice was trained for one day and placed on accelerating rotating rod and the time to fall was recorded. The rotarod test was performed two times each day for five consecutive days. Memory performance was measured on an eight arm radial maze apparatus. Four arms in the maze

contained small pieces of diet and the other four arms were not. If the mouse entered the arm with diet first time it was not recorded as an error, but if they entered the arm without diet, or the arm with diet a second time, this was recorded as one error. Each mouse was tested for five minutes each time. If the mice entered all the baited arms in less than 5 minutes the actual time spent was recorded as the time to complete the test. If they did not visit all 4 baited arms in 5 minutes the completion time was recorded as 5 minutes. All mice were trained for one day and the actual test was performed for five consecutive days. Bone Mineral density was measured by X-ray absorptiometry (Hologic, Discovery A).

Hormone measurements

Blood samples were centrifuged at 3500 rpm for 30 min, and then supernatant was collected as serum, serum leptin and insulin concentrations were measured by using Mouse Leptin ELISA Kit (#90030, Crystal Chem) and Mouse Insulin ELISA Kit (#90080, Crystal Chem) respectively. All procedures were performed according to the manufacturers' instruction. For the measurement of serum leptin and insulin concentration in the AAV injection experiment, leptin ELISA Kit (EZML-82K, Millipore) and Mouse Insulin ELISA Kit (EZMRI-13K, Millipore) were used.

Quantitative RT-PCR

Tissues were put in Trizol (Invitrogen) reagent and homogenized by Bead Ruptor (OMNI). Then total RNA was extracted by chloroform, isopropyl alcohol/RNA precipitation solution (1.2M NaCl & 0.8M disodium hydrogen citrate sesquihydrate) step by step and purified by 75% ethanol. 3 μ g total RNA was used for the cDNA synthesis template (Invitrogen), SYBR Green PCR Kit (TransGen Biotech) was used for Real-time PCR and the quantitative PCR reaction was performed by using 96 well PCR microplate for the Mx3000P Real-Time PCR machine (Agilent), RNA expression data were analyzed by using - $\Delta\Delta C_t$ method. Relative expression levels of all specific genes were normalized to β -actin mRNA expression. Primers were listed in [Table S5](#).

Western blotting

Tissues were homogenized in tissue protein extraction reagent added with a protease, phosphatase inhibitor cocktail and 10 mM PMSF, then lysates were put on ice for 30 min and centrifuged at 12,000 rpm for 10 min. Protein concentration in the supernatant was measured by using bicinchoninic acid (BCA) protein quantification kit. Denatured equal amounts of protein were separated on 10% SDS-PAGE gels and transferred to Immobilon-P PVDF membranes, then blocked in 5% skim milk in PBST (PBS with 0.05% Tween-20) for 1 hour followed by being incubated with primary antibodies at 4°C for 8-12 hours. Unspecific bands on the membranes were washed by using PBST, and then membranes were incubated with HRP-labeled secondary antibodies. The bands were visualized by using ECL blotting reagents (GE Healthcare) and quantified with ImageJ software. The primary antibodies used in this study were anti-eIF2a (#9722, CST), anti-p-eIF2a[Ser51] (#3398, CST), anti-Stat3 (#9132, CST), p-Stat3 (#9134, CST), anti-p70S6K1 (#9202, CST), anti-p-p70S6K1[Thr398] (#9209, CST), anti-S6 (#2317, CST), anti-p-S6[Ser235/236] (#4858, CST), anti-HA (#BE2061, EasyBio), anti-klotho (#ab98111, Abcam), anti-TRPML1 (#ACC-081, Alomone), anti- β -actin (# AB1015T, AmeriBiopharma).

In situ hybridization

All the experiments related to isotopes were performed in a dedicated isotope facility. First, labeled the probe DNA with 35 S, mix 5 μ L 5 \times transcription buffer, 3 μ L rNTP, 1 μ L 0.1 M DTT, 1 μ L RNase inhibitor, 5 μ L DNA probe, 5 μ L DEPC water, 4 μ L 35 S and 1 μ L T7 promoter and then incubated in 37°C incubator for 2 hour, then added 2 μ L DNase and incubated further 30 min. Then filtered small RNA fragments by using chroma spin columns and calculated the concentration. In the next step, prepared the hybridization mixture: containing 80% hybridization buffer (Formamide, 5M NaCl, 50 \times Denhardt's, 1M Tris, 0.5M EDTA and DEPC water) and 20% probe mixture (35 S probe, tRNA, 1 M DTT, DEPC water). For the sections, firstly, fixed the sections in 4% PFA for 20 min then rinsed with PBS for 5 min, then incubated the sections with Triethanolamine (TEA) for 10 min, then also rinsed with PBS for 5 min, at last incubated the sections with each concentration of following graded levels of ethanol (50% -70% -95% -100%). When sections were fully dried incubated sections with hybridization mixture mentioned above at 60°C overnight. On the second day, sections were rinsed step by step in 4 \times SSC (Sodium Citrate), RNAase solution (5M NaCl, 1M Tris, 0.5M EDTA), 2 \times SSC, 1 \times SSC, 0.5 \times SSC, 0.1 \times SSC for 8 min. Once sections were dried, placed sections on paper in film cassette to visualize the bands. The bands were quantified by ImageJ software.

Immunostaining

The brain samples were treated with 4% PFA overnight and then with 30% sucrose solution for 48h at 4°C followed by being embedded with OCT. Sections were fixed in 4% PFA for 20 min and then rinsed with PBS for 5 min, then incubated with 5% BSA (Bovine Serum Abumin) for 1 h followed by being incubated with primary antibodies at 4°C for 8-12 hours. Sections were washed with PBS and then incubated with a secondary antibody for 1h at room temperature. Fluorescence images were obtained by using a confocal microscope (FV1000, Olympus).

Histology

To measure white adipose cell size, 10 μ m frozen sections were fixed with paraformaldehyde (PFA) and incubated in hematoxylin for 1 min before stained with eosin for 30 seconds. Oil red staining was performed to liver cells by staining the sections with oil

red for 5 min then washed with PBS and incubated with 60% isopropanol. At the final step, all sections were sealed with neutral balsam.

Transcriptome data analysis

The hypothalamus of 6 individuals were collected for each diet group, 3 of which were pooled together as one sample, resulting in each group having 2 pooled samples of 3 hypothalamus (Hu et al., 2018). Hypothalamic RNA was extracted as previously described and then sent to Beijing Genomic Institute (BGI) for RNA sequencing. All RNA sequencing was measured by using the BGI-seq 500 sequencer. To determine the sequencing quality of each sample, FASTQ raw data files were measured by using fastQC (www.bioinformatics.bbsrc.ac.uk/projects/fastqc/) quality control tool, after sequencing quality was confirmed, raw reads were aligned to the *Mus musculus* reference genome (GRCm38) using HISAT2-2.1.0 (Kim et al., 2015; Pertea et al., 2016) and Samtools-1.2 modules (Li et al., 2009), and then featureCounts (Liao et al., 2014) tool in Subread-5.0 (Liao et al., 2013) was used to get counts for each sample from BAM files which was obtained from alignment step. To exclude the low counts, only genes with counts per million (CPM) value > 1 were selected for further analysis. Counts were normalized by the trimmed means of M values (TMM normalization) (Robinson and Oshlack, 2010) method in the edgeR (Anders et al., 2013; Lund et al., 2012; McCarthy et al., 2012; Robinson et al., 2010; Robinson and Oshlack, 2010; Robinson and Smyth, 2007) package. To investigate the effects of different dietary protein contents under two fixed levels of fat content on gene expression levels, Generalized Linear Modelling (GLM) function in R-3.5.3 edgeR package was used. GLM model used in this study was: ~P+F+P:F, which means regression against protein (P) and fat contents (F) of diets plus their interaction (P:F). If the interaction effect was not significant ($p > 0.05$), the interaction was not included in the analysis and a revised model (~P+F) was utilized (Hu et al., 2018). To explore genes significantly correlated with dietary protein content respectively under 60% fat and 20% fat conditions, Pearson correlation analysis was performed for normalized log₂-transformed counts of all genes by using Pearson correlation method in R-3.5.3. Then genes significantly correlated with dietary protein content (GLM: $p < 0.05$) respectively in the GLM and Pearson correlation (Pearson: $p < 0.05$ for 60% fat and 20% fat conditions) analysis were selected and loaded into the Ingenuity pathway (IPA) program (Ingenuity Systems; <http://www.ingenuity.com/>) to observe the significantly affected pathways.

Metabolomics measurement and analysis

From each diet group, 10 serum samples were collected, and 5 samples were pooled together as one sample, resulting in 2 pooled samples in each diet group. Serum metabolites were extracted by mixing Chloroform : Methanol : Serum in 1:3:1 ratio and centrifuged at 1,3000 rpm for 3 minutes, supernatant was collected and subject to LC-MS analysis using an Orbitrap™ Exactive™ mass spectrometer at the Glasgow Polyomics facility. Each metabolite was expressed by raw peak intensity, and then these peaks were analyzed step by step using R packages called xcms (Smith et al., 2006), mscombine, missforest (Stekhoven and Bühlmann, 2012), and xmsannotator (Uppal et al., 2017) to match specific mass to charge ratio (m/z ratio) and retention times with HMDB and KEGG databases metabolites. Normalization was performed for raw peak intensities for each sample by using the Metabolomics package (De Livera et al., 2012, 2013; Sysi-Aho et al., 2007), then log₂-transformed. Then Generalized Linear Modelling (GLM) function in R-3.5.3 was used according to following design model: ~P+F+P:F, which means regression against protein (P) and fat contents (F) of diets plus their interaction (P:F). If the interaction effect was not significant ($p > 0.05$), the interaction was not included in the analysis and a revised model (~P+F) was utilized. Pearson correlation analysis was performed for normalized log₂-transformed intensities of all metabolites by using Pearson correlation method in R-3.5.3. Then genes significantly correlated with dietary protein content respectively in the GLM (GLM: $p < 0.05$) and Pearson correlation (Pearson: $p < 0.05$ for 60% fat and 20% fat conditions) analysis were selected and loaded into the Ingenuity pathway (IPA) program (Ingenuity Systems; <http://www.ingenuity.com/>) to observe the significantly affected pathways. Normalized log₂-transformed intensities were used to express the specific metabolite expression levels.

Pair feeding experiment

13 weeks old male C57BL/6N mice were fed with the 1% protein and 60% fat diet, and another group was pair fed (by energy) to this group using the 20% protein and 60% fat diet for two weeks after one week normal diet treatment. Then all mice were given *ad libitum* access to the 20% protein 60% fat diet for 24 hours and their food intakes were recorded.

Intracerebral rapamycin infusion

13 weeks old male C57BL/6N mice were fed with 1% protein 60% fat diet or pair fed with 1% protein 60% fat group by feeding 20% protein 60% fat diet for 2 weeks, and then all mice were treated with DMSO or rapamycin. Anesthetized mice were fixed onto the stereotaxic apparatus and then they were implanted with a brain infusion kit (Alzet) attached to the osmotic pump (with an infusion rate of 0.11 μ l/hr for 4 weeks, Alzet) to the right lateral ventricle (1 mm lateral, -0.34 mm anteroposterior and -2 mm dorsoventral, relative to Bregma) (Yang et al., 2012). Osmotic pumps were filled with DMSO or rapamycin (10mg/nL, LC Laboratories), 10% DMSO (60% PEG400, 30% cremaphor and 10% DMSO) were used in this study, rapamycin was diluted in a mixture composed of 60% PEG400 (Sigma) and 30% cremaphor (Sigma) to make the final concentration of DMSO to 10% (Yang et al., 2012), 10% DMSO was given to the 1% protein and half of the 20% protein pair feeding group, another half of 20% protein pair feeding group was injected with Rapamycin. After 1 week recovery time (during the recovery time, 20% protein group was also pair fed with the 1% protein group), all mice were fed with *ad libitum* 60% fat and 20% protein diet, body weight and food intake were recorded daily

during whole experimental period. After surgery, 3 mice from each group were sacrificed to measure the hypothalamic protein expression.

Intracerebral virus injection

10 weeks old male C57BL/6 mice were intracerebrally injected with adenovirus associated virus (AAV) before treated with special diet, mice were injected right lateral ventricle (1 mm lateral, -0.2 mm anteroposterior and -2.3 mm dorsoventral, relative to Bregma) ([Kleinridders et al., 2009](#)) with control AAV or S6K1 overexpressing AAV ($2 \mu\text{L } 1 \times 10^{12} \text{ pfu}$) with syringes ([Xia et al., 2012](#)), and after two weeks when AAV became active mice were switched to the 60% fat and 1% protein diet. AAV-TRPML1-shRNA and AAV-GCN2-shRNA, AAV- β klotho-shRNA injection experiment were also performed the same as the AAV-S6K1 injection experiment; NTS injection of AAV-S6K1 was performed in the (0.5 mm lateral, -7 mm anteroposterior and -3 mm dorsoventral, relative to Bregma) brain region ([Aklan et al., 2020](#)). All the AAVs used in this study were purchased from Hanbio Biotechnology Co. Ltd. (Shanghai, China)

QUANTIFICATION AND STATISTICAL ANALYSIS

Statistical analysis were performed using the Minitab16, R platform ([R Core Team, 2015](#)) and Microsoft Excel. All values are expressed as mean \pm SD. Average body composition, energy intake, protein intake, physical activity, resting exchange ratio (RER), organ weight, cell size, area under curve (AUC) of glucose tolerance test, relative mRNA expression, protein expression level and maze test performance between different protein content groups were analyzed by one-way ANOVA with Tukey's post-hoc test. Oxygen consumption, energy expenditure, AUC of the glucose tolerance test and frailty test performance were analyzed by using ANCOVA in Minitab 16. ANCOVA with body weight or fat free mass as covariate were performed for oxygen consumption, energy expenditure changes and ANCOVA with fat mass or fat free mass as covariate was used for AUC analysis. Body weight was used as covariate in frailty test ANCOVA analysis. Body weight, food intake and protein expression level comparisons between two groups were performed by Student's t test in Microsoft Excel. To express the relative utilization of each tissue, we used the method of plotting the log transformed final body weight against the final organ weight and then fitted into the linear least regression, if the gradient equals to 1 the organ is being utilized the same rate as the overall body weight, anything greater than 1 is utilized more than body weight and anything between 0 and 1 should be considered protected. Generalized linear modeling and Pearson correlation were used to investigate the dietary protein effect on gene and metabolite expression level, detailed description of analysis can be found in transcriptome and metabolomics data analysis paragraph. $p < 0.05$ was considered as significant in all tests. Data were expressed by $p < 0.05$ (*), $p < 0.01$ (**), $p < 0.001$ (***)

Update

Cell Metabolism

Volume 33, Issue 6, 1 June 2021, Page 1264–1266

DOI: <https://doi.org/10.1016/j.cmet.2021.04.016>

Correction

Very-low-protein diets lead to reduced food intake and weight loss, linked to inhibition of hypothalamic mTOR signaling, in mice

Yingga Wu, Baoguo Li, Li Li, Sharon E. Mitchell, Cara L. Green, Giuseppe D'Agostino, Guanlin Wang, Lu Wang, Min Li, Jianbo Li, Chaoqun Niu, Zengguang Jin, Anyongqi Wang, Yu Zheng, Alex Douglas, and John R. Speakman*

*Correspondence: j.speakman@abdn.ac.uk

<https://doi.org/10.1016/j.cmet.2021.04.016>

(Cell Metabolism 33, 888–904.e1–e6; May 4, 2021)

In the original version of the article's Figure 7, the Figures 7P and 7O are the same. We mistakenly duplicated the figure 7P during the production process. This error has been corrected online. As this error occurred in figure production and not during data analysis, this error has no impact on the main results or conclusions of this publication. The authors apologize for this error and any confusion it may have caused.



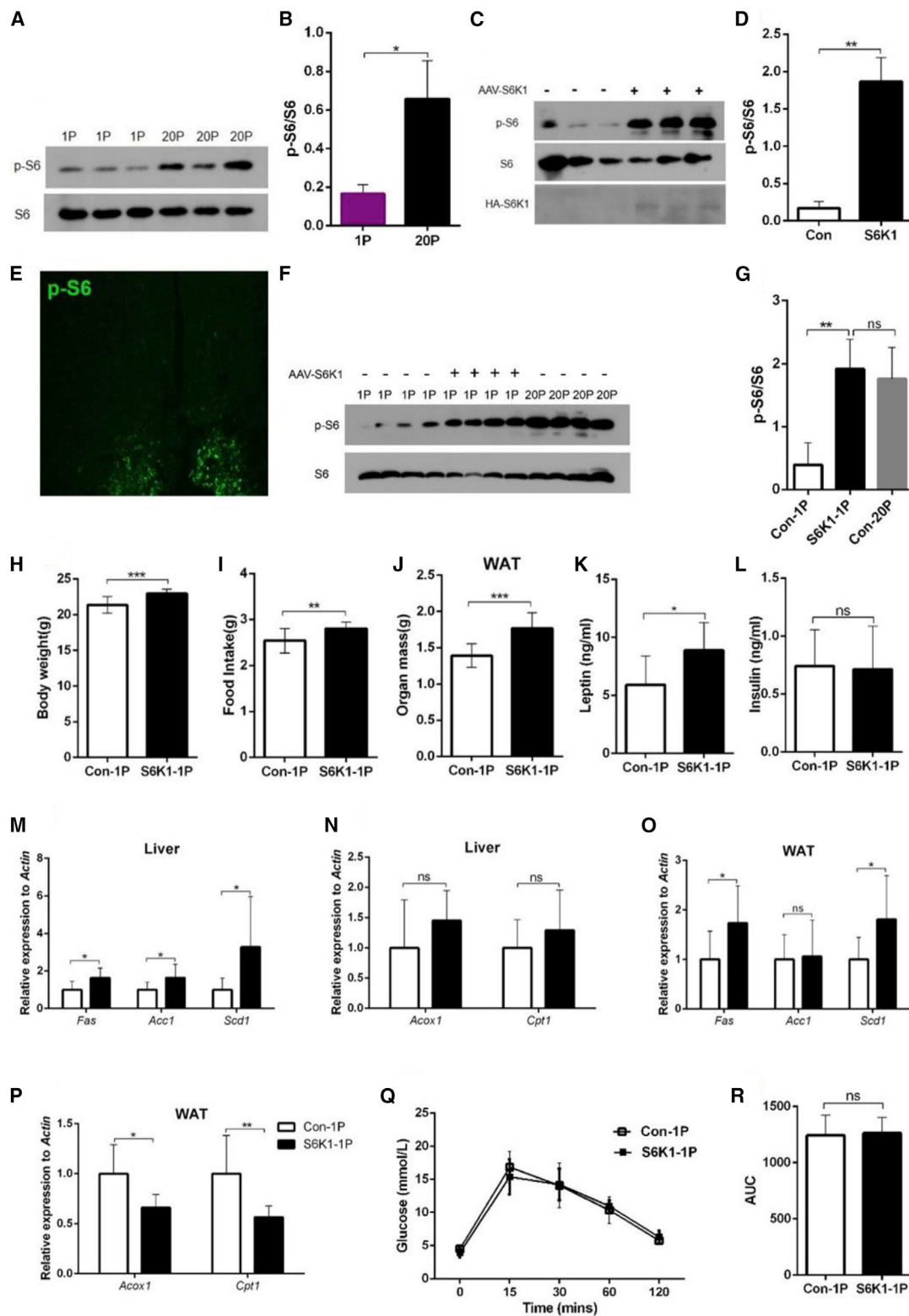


Figure 7. Reduced food intake and body weight of the 1% protein diet is partially dependent on the mTOR signaling pathway (Corrected)

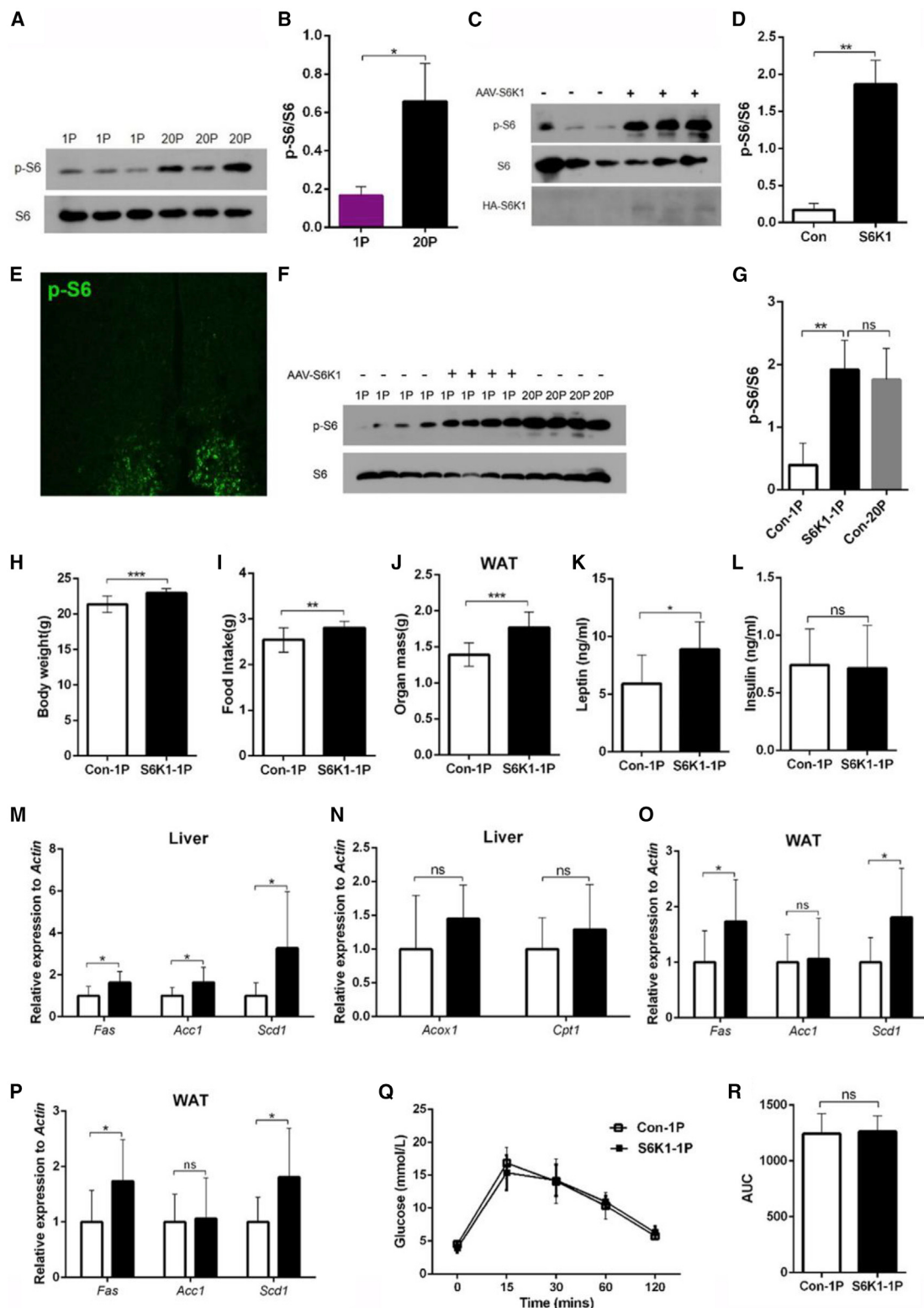


Figure 7. Reduced food intake and body weight of the 1% protein diet is partially dependent on the mTOR signaling pathway (Original)